

REVIEW ARTICLE

Detection of biomarkers using recombinant antibodies coupled to nanostructured platforms

Michael R. Kierny, Thomas D. Cunningham and Brian K. Kay*

Department of Biological Sciences, University of Illinois at Chicago (UIC), Chicago, IL, USA

Received: 24 January 2012; Revised: 30 May 2012; Accepted: 9 June 2012; Published: 23 July 2012

Abstract

The utility of biomarker detection in tomorrow's personalized health care field will mean early and accurate diagnosis of many types of human physiological conditions and diseases. In the search for biomarkers, recombinant affinity reagents can be generated to candidate proteins or post-translational modifications that differ qualitatively or quantitatively between normal and diseased tissues. The use of display technologies, such as phage-display, allows for manageable selection and optimization of affinity reagents for use in biomarker detection. Here we review the use of recombinant antibody fragments, such as scFvs and Fabs, which can be affinity-selected from phage-display libraries, to bind with both high specificity and affinity to biomarkers of cancer, such as Human Epidermal growth factor Receptor 2 (HER2) and Carcinoembryonic antigen (CEA). We discuss how these recombinant antibodies can be fabricated into nanostructures, such as carbon nanotubes, nanowires, and quantum dots, for the purpose of enhancing detection of biomarkers at low concentrations (pg/mL) within complex mixtures such as serum or tissue extracts. Other sensing technologies, which take advantage of 'Surface Enhanced Raman Scattering' (gold nanoshells), frequency changes in piezoelectric crystals (quartz crystal microbalance), or electrical current generation and sensing during electrochemical reactions (electrochemical detection), can effectively provide multiplexed platforms for detection of cancer and injury biomarkers. Such devices may soon replace the traditional time consuming ELISAs and Western blots, and deliver rapid, point-of-care diagnostics to market.

Keywords: *phage-display; scFv; Fab; therapeutic antibody; affinity maturation; mutagenesis; nanotechnology; carbon nanotube; nanoshell; electrochemical detection*

Michael Kierny and Thomas Cunningham contributed equally



Brian Kay Professor Brian Kay did his undergraduate studies at the University of Chicago and graduate work at Yale University. He then held academic appointments at University of North Carolina-Chapel Hill, University of Wisconsin-Madison, and Argonne National Laboratory, before joining the Department of Biological Sciences at the University of Illinois at Chicago, where he has been the last six years. His lab is currently using phage-display to generate affinity reagents (i.e., antibody fragments, peptide ligands, fibronectin fragments) to bacterial and eukaryotic proteins. He has authored over 150 scientific reports and reviews, co-edited three books, and been issued 15 patents.



Thomas Cunningham graduated with his Bachelor's degree in Immunology from the department of Molecular and Cell Biology at the University of California-Berkeley. After receiving his PhD in Biochemistry at the University of Illinois Urbana-Champaign he joined Brian Kay's lab at the University of Illinois at Chicago to isolate affinity reagents using recombinant antibody techniques, like bacterial phage-display. He currently manages operations at a large antibody manufacturer in the California biotech community and maintains an avid interest in the antibody engineering field.



Michael Kierny received his Bachelor's degree in Biology from Iowa State University in 2006. He worked in the lab of Dr. Marit Nilsen-Hamilton through his undergraduate career. After graduation, he continued to perform research at this laboratory and also for the U.S.

One of the driving forces in basic and applied science has been the search for biomarkers, such as proteins, post-translational modifications, peptides, or metabolites, which are unique and representative of a particular cell type or disease state. In the ideal case, these would be biomarkers that are released from the source in sufficient amounts to be easily detected in complex mixtures, like serum or saliva. (Fig. 1a). Protein biomarkers are the most common type of biomarker used in medical diagnostics. The discovery process (Fig. 1b) for protein biomarkers has been dominated by the use of liquid chromatography fractionation in conjunction with tandem mass spectrometry (LC/MS/MS) (1–3). This method has been successful because it can separate and identify thousands of proteins from a single complex sample that has been digested with

Department of Energy Ames Laboratory. In 2007 he joined the Biological Sciences PhD program at the University of Illinois at Chicago. He is currently in Brian Kay's lab conducting research related to the detection of biomarkers for retinal injury using scFv recombinant antibodies generated using phage-display.

a protease to yield short, traceable peptides (Fig. 1c). Following a comparison of a diseased to a healthy subject's profile, one can identify the proteins that are correlated to the diseased state, which in most cases for biomarkers have a concentration in the nanogram per milliliter range (4). The proteins or peptides are then used as targets in antibody selection schemes (Fig. 1d) to generate detection reagents. After these biomarkers are

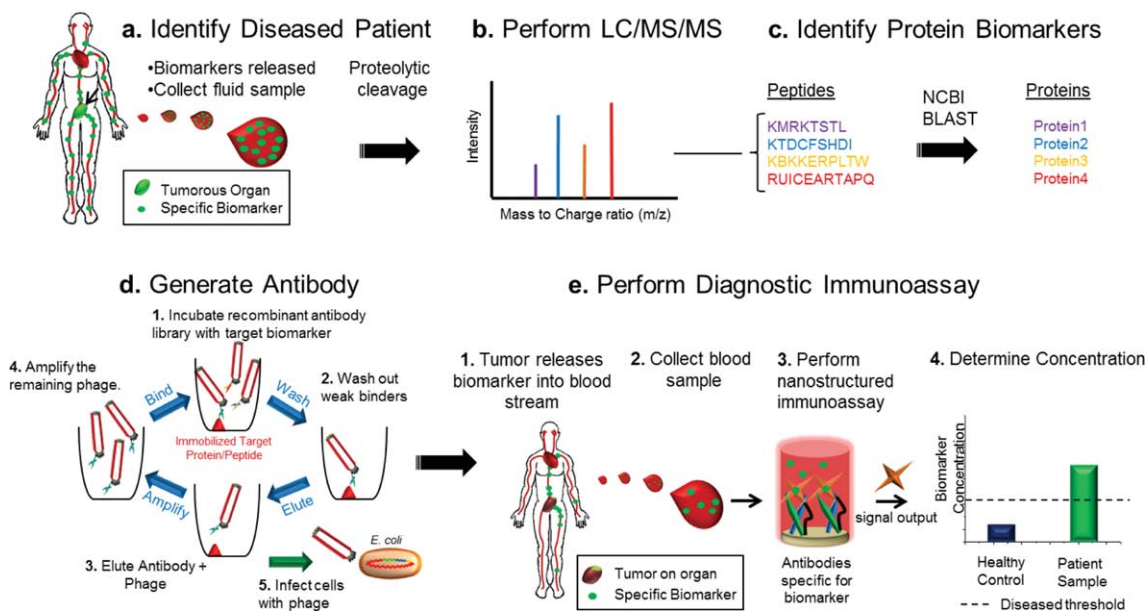


Fig. 1. From biomarker discovery to disease diagnosis. (a) Specific proteins are released into circulation in response to developing disease or injury. Shown here is cancer growth on an organ (arrow), such as the prostate gland, releasing biomarkers (green spheres) that enter the blood stream, where they circulate before eventually being cleared. To determine the biomarkers present, the serum is collected from a diseased individual and subjected to trypsin digest to generate many short peptides. (b) The sample is then separated using liquid chromatography, and fractions are analyzed by tandem mass spectrometry where fragment ions of the peptides result from collision-induced dissociation. The mass-to-charge ratio of the fragments are used to determine the amino acid sequence of a charged peptide (3). (c) A database, such as GenBank at the National Center for Biotechnology Information (NCBI), is searched with a bioinformatics program like BLAST (Basic Local Alignment Search Tool) using the amino acid sequence to identify the full length protein. Comparison of the diseased serum protein profile to a healthy profile will elucidate the biomarker protein. (d) The full protein or a synthesized peptide is used in a phage-display selection to generate specific recombinant antibodies. 1. The phage-display library is incubated with the target protein or peptide. 2. The weak binding antibodies are washed away. 3. The tight binding antibodies are retained and eluted. 4. The antibody-displaying phage are amplified through infection of bacteria. The process is then repeated under more stringent conditions. 5. Single colonies of phage infected *Escherichia coli* are sequenced and the antibodies characterized. (e) A diagnostic immunoassay is performed on serum from a patient with suspected early onset of disease. 1. The tumor is releasing low amounts of biomarker protein into the blood stream. 2. A sample of blood is collected and prepared. 3. Using the previously generated recombinant antibodies, the biomarker is recognized when the blood serum sample is introduced into a nanostructured immunoassay. Depending on the platform, a signal is produced that is proportional to the concentration of the biomarker. 4. The concentration is determined, compared to healthy controls, and a diagnosis made. Certain concentrations of a particular biomarker may be indicative of a disease or injury. This can lead to additional tests that are more invasive to the the patient.

validated to be indicative of a particular disease, an accurate diagnosis can typically be made immunologically on a nanostructured platform, or once again through mass spectrometry (Fig. 1e). While one would ideally prefer to find a single biomarker that is representative of a cell state or disease, it is likely that combinations of biomarkers will be needed to make a confident assessment.

Currently, there are a number of biomarkers known to be associated with certain states of human health and disease. These include human chorionic gonadotropin (hCG) in urine and serum (for monitoring pregnancy) (5), alpha-fetoprotein (AFP) in amniotic fluid (as an indication of neural tube defects) (6), cardiac troponin I (cTnI) in blood (to monitor acute myocardial infarction in patients) (7), and a panel of five biomarkers including alpha-II Spectrin Breakdown Product (SBDP) (to diagnose traumatic brain injury) (8, 9). Many types of cancer are evaluated to some degree by the occurrence of biomarkers. These include Carcinoembryonic antigen (CEA) for colon and rectal cancers (10), cancer antigen 125 (CA125) for ovarian cancer (11), Prostate-Specific Antigen/Kallikrein 3 (PSA/K3) for prostate cancer (12), and Human Epidermal growth factor Receptor 2 (HER2/Neu) for breast cancer (13, 14).

Antibodies are commonly used to locate and quantify individual proteins in complex mixtures and tissues. Often the amount, activity, or location of a particular protein changes over time with genetic mutation, infection, or disease, thus antibodies are extremely useful in monitoring individual proteins. In the past, antibody production was triggered upon presentation of an antigen to a host's immune system. Polyclonal antibodies, purified from the serum of an immunized animal (i.e. mouse, rabbit, goat, etc.), or monoclonal antibodies, secreted by immortalized B cells from the spleen of an immunized animal (15) are commonly used in immunological assays. This is in contrast to newer methods that involve the generation of large libraries of recombinant antibodies or scaffolds that are engineered to behave like antibodies, and then screening said libraries *in vitro* for the desired binding properties. The advantages of using recombinant antibodies will be discussed below.

Recombinant antibodies

Recombinant antibodies have many attractive attributes compared to the traditional polyclonal antisera and monoclonal immunoglobulin antibodies. First, they can be overexpressed and easily purified in a range of common eukaryotic and prokaryotic hosts. Second, the genotype and phenotype of the antibody can be linked through various display technologies, allowing for the easy recovery of the coding regions of recombinant antibodies. Third, by depositing the sequence information in GenBank any researcher can renew clones through gene synthesis. Third, the sequence information

allows for subcloning and bioengineering to generate fusions with fluorescent proteins or enzymes. Fourth, they can be tagged with epitopes or short peptide sequences, without interfering with their binding properties. Fifth, unlike antibody generation through immunization, researchers can select for recombinant affinity reagents that work in the presence of certain salts, buffers, detergents, at a particular pH, etc. Furthermore, through the process of subtraction, one can develop antibodies that recognize specific epitopes (regions of the protein), post-translational modifications, and conformations. The increased throughput (16) over rabbit or mouse monoclonal antibody generation has made it technically feasible to attempt to analyze the >20,000 proteins that comprise the human proteome (17). Finally, with recombinant antibodies, the knowledge of the DNA sequence and the ease at which it can be manipulated allows for unique studies. For example, antibodies have been expressed in cell lines, where they can interact with their cell target (18, 19), their affinity can be improved through directed evolution under increased selection pressures (20, 21), they can be used to inhibit signaling pathways to study organism development (22), they can serve as the basis of complex biosensors (23), and they can be designed to incorporate unnatural amino acids, thereby increasing the range of molecular interactions by which they may bind their targets (24).

Many of these attributes make recombinant antibodies especially well suited for incorporation and fabrication into nanostructured devices. They can be engineered to include short peptide extensions, such as the AviTag, which serves as a substrate for a biotin ligase to add a single biotin molecule (25). This form of post-translational modification does not interfere with the antibody's function, as sometimes is the case with chemical biotinylation. The attached biotin allows for orientation-specific attachment of the antibodies to nanostructures through the streptavidin linkage, and guarantees that 100% of the antibody molecules can bind to antigen, which allows lower detection limits to be reached, and yields more reliable assays. Other methods for orientation-specific immobilization can be made through amino acid replacement or addition of a cysteine residue and subsequent attachment to gold-coated surfaces (26).

Introduction of free cysteine residues or biotin can also serve as the starting point for the attachment of DNA oligonucleotides, which permits Proximity Ligation Assay (PLA) (27), an assay that combines the protein recognition capabilities of an immunoassay with the amplification power of the Polymerase Chain Reaction (PCR). Two antibodies against the same antigen can be tagged with unique oligonucleotides, where upon binding, the oligonucleotides are brought in close proximity to one another where they can be ligated together through

the presence of a splint oligonucleotide. The ligated DNA molecule can then serve as a template for PCR or Rolling Circle Amplification (RCA), thereby allowing *in situ* detection of antigen recognition in cells or tissues (28). This method can also be used for highly sensitive detection of biomarker proteins in solution (29, 30).

Another advantage of a recombinant antibody is that its binding can be altered through point mutations to either eliminate binding to an antigen (for use as a negative control) or to fine tune its binding or specificity. It has been shown that tumor penetrating efficiency is reduced for scFv antibodies that have a very high affinity (K_d values of 1 nM to 10 pM), due to their long off rate kinetics for the initial antigen interaction occurring at shallow depths. Antibody penetration depth actually increases when affinities are lowered to 100 nM through mutation (31). The success of tumor targeting of antibody-coupled nanostructures will depend on the ability of complexes to diffuse through the tissue to reach its antigen.

Types of recombinant antibodies

Immunoglobulin isotype G (IgG) antibodies are composed of two heavy and two light chains (Fig. 2a). Diversity in antibody–antigen interactions is achieved through the interaction of six short (3–25 amino acids)

complementarity determining regions (CDRs), within the variable domains of the antibody heavy and light chains. Fragments of antigen binding (Fabs) (Fig. 2b) and single chain fragments of variation (scFv) (Fig. 2c) represent structurally minimized versions of full-length human antibodies and, as such, are popular formats in recombinant antibody technology. The scFv consists of the variable domains (i.e. V_H , V_L) of both heavy and light chains that have been combined into a single polypeptide (32, 33). ScFvs are well suited for molecular biology because they can be cloned and manipulated as individual polypeptides, and can be displayed on the surface of bacteriophage (phage), while still retaining selective binding to antigens. As shown in Fig. 2c, the antigen-binding surfaces of the heavy and light chains can be connected *via* a 15 amino acid linker. In addition, such scFv molecules can be tagged at their C-termini with the c-myc epitope and six histidines, permitting detection and purification, respectively. Even though these antibody fragments are significantly smaller (25 vs. 150 kDa) than IgGs, they can still bind their respective antigens tightly (i.e. with dissociation constants of 5 μ M to 10 nM), and are amenable to directed evolution (34) for improvement of their affinity. Fab antibodies (Fig. 2b) are \sim 50 kDa, which is twice the size of scFvs, and are composed of two

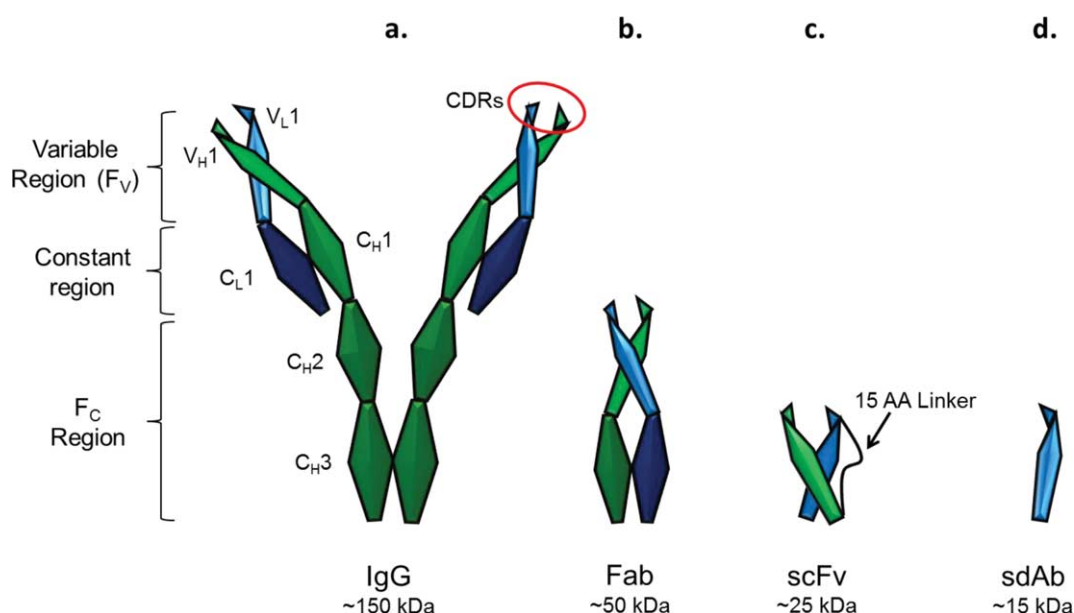


Fig. 2. Molecular formats of antibodies. (a) Immunoglobulin subtype G (IgG): full size antibody molecule, which is secreted by B cells of the mammalian immune system. The variable domains (V_L and V_H) contain six complementarity determining regions (CDRs), which contact the antigen. Constant regions (C_H , C_L) provide stable interactions between the light and heavy chains. The Fragment of the constant region (Fc) triggers a physiological response by interacting with Fc receptors of cells. The IgG molecule is bivalent and can simultaneously recognize two identical antigen molecules. (b) Fragment of antigen binding (Fab): Composed of the light chain and half of the heavy chain; the two chains are held together *via* disulfide bonds. The Fab is monovalent, and can recognize only one antigen molecule at a time. (c) Single-chain Fragment of variation (scFv): The variable domains of the heavy and light chains can be joined through a flexible 15 amino acid long linker. The scFv is monovalent, recognizing one antigen molecule at a time. (d) The single-domain antibody (sdAb) is devoid of light chains and can be derived from camelids V_{HH} antibodies.

polypeptides with constant regions linked through disulfide bonds. Fabs are monovalent and, in contrast to scFvs, generally resistant to aggregation. Affinity maturation and selection techniques are similar to that of scFvs, but conversion of a Fab to and from an IgG is straight forward since the highly conserved constant region allows the layout of the variable domain to remain unchanged (35). Finally, single-domain antibodies (sdAb) (Fig. 2d), such as those derived from V_{HH} immunoglobulins present in camelids, lack the V_L domain and consist just of the V_H domain (36). Such antibody fragments are advantageous because of their small size, ~ 15 kDa, they are readily expressed in bacteria, and they penetrate deep into tissues after being introduced into patients (37).

Other types of scaffold proteins

In contrast to the use of antibody fragments for generating affinity reagents, one can use alternative scaffolds. One such example is the fibronectin type III domain of the glycoprotein fibronectin. It is an extracellular matrix ligand binding protein that has six loops of which three have been randomized and displayed on phage to generate a library (38). DARPins are another set of repurposed scaffolds designed from the ankyrin repeats (39, 40) that are normally involved in mediating protein interactions. Here, repeats of two alpha-helices joined by a loop are linked by beta-hairpins to one another in a modular fashion to form a 2–3 repeat binding pocket with N- and C-terminus ankyrin caps. Affibodies also originate from a protein unrelated to antibodies or antibody fragments. These are composed of the Z-domain in the cell wall protein A, of the *Staphylococcus aureus* bacterium, that has two randomized alpha-helices for interaction with a target protein (41). Libraries of scaffold variants can be constructed through molecular biology techniques, and then screened through multiple rounds of affinity to yield tight, binding clones. This procedure yields a renewable, *in vitro* generated affinity reagent that has high specificity and affinity to a given antigen (42–45).

Display technologies

In vitro screening methodologies benefit from the development of faster and more efficient ways to ‘test’ candidate reagents when presented to a given ‘target’. DNA and RNA based affinity reagent selection systems like the evolution of single-stranded DNA or RNA aptamers, by SELEX (Systematic Evolution of Ligands by Exponential enrichment), select for nucleic acids with a tertiary structure that bind specifically to analytes (46–48). For display technologies, affinity reagents often are antibodies, antibody fragments, peptides and even DNA and RNA. While DNA (49) and RNA (50) based affinity reagents do not require a host, antibody and peptide

based affinity reagents require a system to express or display prior to selection. These include ribosome and mRNA-display (51), yeast-display (52), bacterial-display (53) and phage-display (54), where antibodies, and fragments of antibodies (scFv, Fab, $F(ab)_2$) are expressed on the surface of cells or, as in phage-display, where they are synthesized on the envelope of the viral phage (55). Ribosome and mRNA-display, as *in vitro* display techniques, are capable of selecting extremely high affinity reagents by incorporating mutations in each round of selection (56). Phage-display requires a secondary mutagenic library to be constructed after the initial rounds of selection from the naïve library, to obtain the highest affinity reagents (57). For the sake of brevity, this review will focus on the utility of scFv antibodies that have been generated by phage-display.

Phage-display

In phage-display, antibody fragments, cDNA segments (complementary DNA), or combinatorial peptides are expressed as fusions to a capsid protein present on the surface of viral particles. While bacteriophage M13 is the most commonly used vector for phage-display, λ , T7, retrovirus, and baculovirus have also been used. Phage-display offers the following conveniences: [1] the peptide or proteins, which are expressed on the surface of the viral particles, are accessible for interactions with their targets; [2] the recombinant viral particles are stable; [3] the viruses can be amplified, and [4] each viral particle contains the DNA encoding the recombinant library member on the surface of that viral particle, thereby providing a physical linkage between the genotype and phenotype. Thus, phage libraries are conveniently screened by affinity selecting viral particles that bind to targets, propagating the recovered phage particles, and sequencing the DNA inserts of clonal isolates. Usually three rounds of selection are sufficient to screen a phage-display library, with binding clones confirmed in an enzyme-linked immunosorbent assay (ELISA) (58).

Typically, scFvs are displayed as fusions to the N-termini of coat proteins pIII or pVIII of bacteriophage M13. Phage particles are composed of circular, single-stranded DNA, which is surrounded by a cylinder of coat proteins (Fig. 3). Most of the viral capsid consists of the major coat protein pVIII, of which there are $\sim 2,700$ copies per phage. At one end of the phage particle, there are five copies each of pIII and pVI that are involved in host-cell binding and in the termination of the assembly process, respectively, whereas the other end contains five copies each of pVII and pIX, which are required for the initiation of assembly and for maintenance of virion stability, respectively (59). Traditionally, both pIII and pVIII have been used to display peptide and antibody fragments. Large, non-immune or ‘naïve’

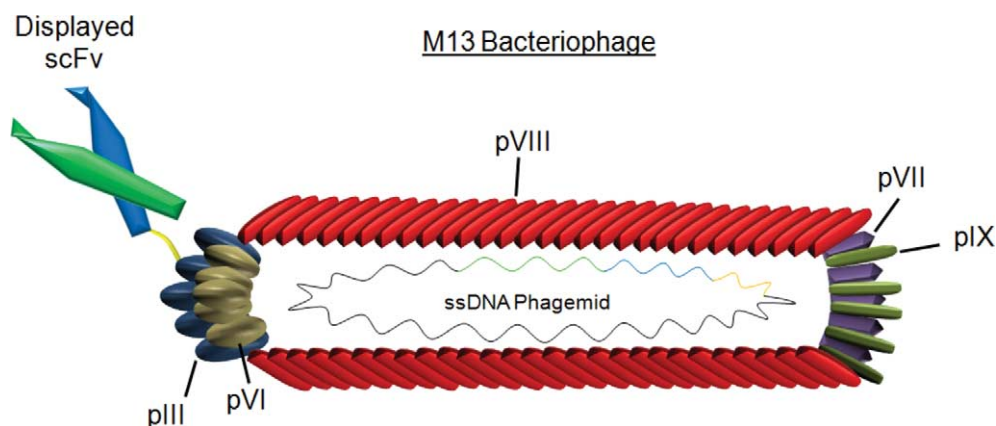


Fig. 3. Phage-display using M13 bacteriophage. As shown here, a phage particle displays an scFv fused to the N-terminus of the minor coat protein, pIII, through a short peptide linker. The major coat protein, pVIII, encapsulates the single-stranded DNA (ssDNA) viral genome that encodes the genes for scFv and pIII. While five molecules of pIII are expressed per phage particle, typically zero or one copy of the scFv is actually displayed. When using a phagemid genome for display of scFvs, proteins pVI, pVII, pVIII, and pIX are supplied by a helper phage genome that is present inside the *Escherichia coli* cell.

antibody libraries displayed on pIII, have proven to be a general method to readily isolate high affinity and specific human antibodies against a variety of target antigens (60, 61). In addition, pVII and pIX can be used to display V_H and V_L domains, respectively; this form of heterodimeric presentation yields a viable fragment of variation (Fv) with fully functional binding and catalytic activities (62). It is also possible to display human scFvs (63) and Fabs (64) fused to the N-terminus of pIX.

Phage-display selection procedures

The key procedural advantage of phage-display is the linkage between an antibody's genotype (DNA sequence encapsulated in the phage particle) to its phenotype (specificity and affinity of the phage-displayed antibody). The selection procedure is fast and operates on sequential rounds of display and enrichment of target specific antibody binders (Fig. 1d). Three rounds of selection are sufficient to isolate and amplify the strongest binders while removing non-specific, non-binding clones. The first round of selection is most important, as the entire library of affinity reagents is introduced to the target. A subset of target specific binders stay bound to their respective epitopes while the majority of the phage library containing nonspecific binders is washed away. Recovered phage particles are then eluted to infect bacteria, which are amplified in selective media. Elution of specific phage can be performed different ways, with extreme pH (i.e., pH 2 or 12) and protease cleavage (i.e., trypsin) (65, 66) being the most common. It is also possible to introduce a protease cleavage site in the target (67) so only target-bound phage particles are released. With an intact target and naïve library in hand, three rounds of selection can be carried out in a little over 1 week.

Target presentation is critical to finding the best binder in a library. Selection methods fall into two categories of

antigen presentation; solid support and in solution. Solid phase selections, or biopanning, immobilize the target to a solid support, for example, by adsorption to the well of a plate or the attachment to a column (68). In-solution selections depend upon affixing the target to a freely moving particle in solution, like paramagnetic beads or live cells (69, 70). Protein and non-protein targets can be biotinylated *in vitro* or *in vivo* for presentation on neutravidin or streptavidin coated beads or plates (71). Specific enzymatic biotinylation *in vivo*, through the use of the AviTag, is a common strategy for optimal target presentation (72, 73).

Affinity maturation using phage-display

It is important to note that many antibody properties (specificity, thermostability, protein expression, etc.) can also be selected through variant or affinity matured library generation, although increased affinity is often the initial primary characteristic. The affinity of antibodies generated by animal immunization generally ranges between 50 nM and 100 pM (74, 75). However, *via* directed evolution, it is now possible to lower antibody binding constants to the low picomolar and mid-femtomolar range (20). The affinity of an antibody isolated from an initial screen can be increased two to three orders of magnitude to that of the original sequence using affinity maturation techniques based on display technology (76–79).

The focus of recombinant antibody affinity maturation strategy involves pairing optimum heavy and light chain variable regions. Display technology allows one to quickly create large libraries of mutant clones by PCR (random or directed). These mutated sequences are then displayed on filamentous phage and screened for improved binding. Recently, the size of a matured library has been correlated with the optimum K_d of the best

binder from that library (80). Two types of antibody diversification techniques predominate; chain shuffling and mutagenesis. Chain shuffling involves fixing the DNA sequence of one of the two chains (V_H or V_L) and combining with a library, or repertoire, of complementary chains to yield a library from which an optimum chain combination can then be selected from. Chain shuffling can be performed using a fixed V_H or V_L , although a fixed V_H is often shuffled with a library of V_L s due to the fact that the V_H of an antibody contributes the bulk of the binding energy (81). Through chain shuffling, large improvements in affinity have been observed (82–84). Mutagenesis of the antibody DNA sequence yields mutant antibody variants, which when displayed on phage, can be selected for depending on the desired characteristic (increased affinity, thermostability (85, 86), increased expression, etc.). This is commonly achieved by error-prone PCR (87) or through the misincorporation of nucleotides (88).

From an affinity standpoint, this kind of approach can be used to select for mutations across the entire length of the scFv (not just the crucial CDR's) that enhance the affinity of an antibody for its antigen. This increased affinity may result from the relief of steric hindrance, the promotion of a more compact structure, etc. Systematically directing the mutagenesis towards the variable regions (CDR's) to increase an antibody's affinity is also an option (89). Direct mutagenesis, in conjunction with alanine-scanning and epitope modeling, can help pinpoint the residues most critical for antigen binding.

Examples of phage-display derived therapeutic antibodies

Since emerging in the early 1990s (90), phage-display has proven to be a powerful tool for therapeutic antibody development. There are several examples of phage-display derived antibodies currently used as therapeutics. The US Food and Drug Administration (FDA) has thus far approved two and, as of 2010, there are 25 therapeutic antibodies in clinical trials for human therapeutic use. It is interesting to note that of the 131 monoclonal antibodies developed for therapeutic use between 2001 and 2008, nearly 27% were phage-display derived recombinants (91, 92).

Adalimumab (Humira[®], Abbott Laboratories) (93) is the first therapeutic antibody derived from phage-display technology. Approved by the FDA for rheumatoid arthritis in 2003, it is now poised to become 2012s best selling drug in the world (94). This human antibody antagonizes the pro-inflammatory activity of the cytokine, tumor necrosis factor alpha (TNF- α). Adalimumab binds specifically, and with high-affinity ($K_d=100$ pM), to TNF- α and neutralizes its activity ($IC_{50}=130$ pM) (95). Adalimumab was created through phage-display, using

guided selection from a mouse monoclonal antibody. This method involves transitioning the mouse sequences to human *via* various chimeric forms (96, 97). The heavy and light variable chains of the mouse antibody were converted to scFv format and split to pair with a complementary human light or heavy variable region. These human heavy and light variable chain sequences were then combined and continually selected for with TNF- α . After transitioning the scFv to an IgG, Adalimumab exhibits low immunogenicity and has a serum half-life of 10–20 days (98). Currently, Adalimumab is prescribed to treat rheumatoid arthritis, Crohn's disease, psoriasis, arthritis and ankylosing spondylitis.

The second therapeutic to be generated from a phage-display library of scFvs is the monoclonal antibody Belimumab (Benlysta[®]), a B-lymphocyte stimulator (BLyS) inhibitor (99, 100). Belimumab inhibits the function of BLyS, tumor necrosis factor superfamily member 13b (TALL1), which is a cytokine known to regulate B cell proliferation and differentiation, by binding to its three receptors TACI, BCMA, and BAFFR (101). Inhibition of this cytokine cell signaling causes an increased number of autoreactive B-cells to undergo programmed cell death, thereby reducing the formation of auto-antibodies and providing relief for patients suffering from autoimmune diseases (102). Recent FDA approval of Belimumab for the treatment of Systemic Lupus Erythematosus (SLE) is the first new therapy for this autoimmune disease in 56 years (103). Phase III clinical trials of the drug showed efficacy and safety by reducing SLE disease activity and, in some cases, decreased the frequency of flares, as compared to placebo (104). The antibody, known as LymphoStatB, was selected through a screen of a naïve phage-displayed scFv library with a diversity of 10^{10} – 10^{11} . Affinity maturation, using random mutagenesis by PCR, and then subsequent conversion into a full IgG, yielded an antibody that bound tightly to and inhibited BLyS in an immobilized assay, with an effective concentration at half maximum (EC_{50}) value of 0.02 nM and, an in solution inhibitory concentration at half maximum (IC_{50}) value of 8 nM. In addition, cross reactivity with TNF- α or any other closely related protein was minimal. The specificity, binding strength, long half-life, and cytokine neutralizing ability of the antibody lend to a potentially successful therapeutic for many autoimmune disorders (105).

Given the contributions to therapeutic antibody development over its short history, phage-display has been shown to be a future source of therapeutic affinity reagents. Phage-display offers the advantage of working with human antibody sequences, as well as a quick, yet powerful tool to affinity mature first generation binders, and thus has become an accepted source for human antibody therapeutics.

Microarray technology

Microarray ('chip') technologies were commercialized in the mid to late 1990s by companies (106, 107) for the detection and quantitation of disease and biomarker genes. These nucleic acid-based micro- and nano-scale arrays allow researchers to quickly and quantitatively measure the entire expression profile of a disease state, or a targeted subset of fully customizable target genes. Due to issues like reagent stability and advances in DNA synthesis technology, nucleic acid-based arrays have matured faster than their protein-based counterparts. Like nucleic acid-based arrays, protein- or antibody-based arrays hold the promise of sensing targets of interest on a systems level, but are inherently more complex due to the increased variability of the proteome compared to the genome. Nevertheless, antibody-based arrays have the exciting potential to further identify biomarkers and aide in diagnosing disease (108, 109).

Nanostructured biosensor platform technologies

In the second half of this review, we highlight several recent publications that utilize engineered antibodies in nanostructured sensors to detect biomarkers of disease or injury (Table 1, Fig. 4). However, as both the fields of nanotechnology and synthetic antibody generation are relatively new, there have not been enough studies to completely adhere to these criteria. Therefore, when necessary, we have discussed nanotechnologies that have not yet implemented engineered antibodies or been used to detected biomarkers of disease, but show an obvious connection to this end. We also describe some novel micro-scale technologies that have been adopted for sensing of protein biomarkers (Fig. 5). In the past, biomarkers were detected by ELISA (110), Western blotting (111), and mass spectrometry (112), which are labor intensive and time consuming techniques. Nanostructured platforms offer

Table 1. Nanotechnologies used to detect protein biomarkers of disease. A list of published nanotechnologies and signal outputs that use monoclonal or recombinant antibodies to detect biomarkers in solution or in tissue

Technology	Antibody type	Signal output	Analyte	Detection details	References
SWCNT	IgG	Electrical conductivity	Chromogranin A (CgA)	100 pM–1 nM (5 ng/mL–50 ng/mL)	(123)
Ni coated SWCNT	scFv	Electrical conductivity	Carcinoembryonic antigen (CEA)	10 ng/mL	(122)
CNT	scFv	Electrical conductivity	Osteopontin (OPN)	1 pg/mL	(124)
SWCNT forest	IgG	Electrochemical redox	Interleukin-6 (IL-6)	30 pg/mL	(115)
MWCNT-HRP	IgG	Electrochemical redox	Interleukin-6 (IL-6)	0.5 pg/mL	(117)
Gold nanosphere	IgG	SERS	Carcinoembryonic antigen (CEA)	1 pg/mL–100 ng/mL	(135)
Gold nanosphere	IgG	SERS	Angiogenin (ANG)	0.1 pg/mL	(136)
Gold nanosphere	IgG	SERS	Alpha-fetoprotein (AFP)	1.0 pg/mL	(136)
Gold nanoparticle	scFv	SERS	Endothelial growth factor receptor (EGFR)	30 mm ³ tumor detection	(138)
Gold nanoshell	Fab	SERS	Calcium Channel Voltage-Dependent α -1F (CACNA1F)	~20 ng (10 ng/ μ L)	(137)
QCM	IgG	Δ Resonance frequency	Prostate Specific Antigen (PSA)	290 pg/mL in serum	(157)
QCM	scFv	Δ Resonance frequency	Cytochrome P450 1B1 (CYP1B1)	130 ng/mL	(160)
CdSe/ZnS quantum dot	scFv	Photoluminescence	Human Epidermal growth factor Receptor 2 (HER2)	Imaged breast cancer cell line MCF7	(150)
CdSe/ZnS quantum dot	scFv	Photoluminescence	Prostate Specific Cancer Antigen (PSCA)	Imaged breast cancer cell line MCF7	(150)
CdSe/ZnS quantum dot	SdAb	Photoluminescence	Endothelial growth factor receptor (EGFR)	Imaged breast cancer cell line SK-BR3	(154)
Quantum dot	scFv	Diffuse Fluorescence Tomography (DFT)	Human Epidermal growth factor Receptor 2 (HER2)	Whole-body tumor imaging	(155)
Silicon nanowires	IgG	Electrical conductivity	PSA; CEA; Mucin-1	75 fg/mL (2 fM); 100 fg/mL (0.55 fM), 75 fg/mL (0.49 fM)	(144)
Si ₃ N ₄ microcantilever	IgG	Cantilever deflection	PSA	200 pg/mL–60 μ g/ml in serum	(168)
Microcantilever	IgG	Resonance frequency	PSA	10 pg/mL	(169)
Microcantilever	scFv	Cantilever deflection	Peptide	20 ng/mL (1 nM)	(26)
Microcantilever	Fab	Cantilever deflection	HER2	2 ng/mL	(170)

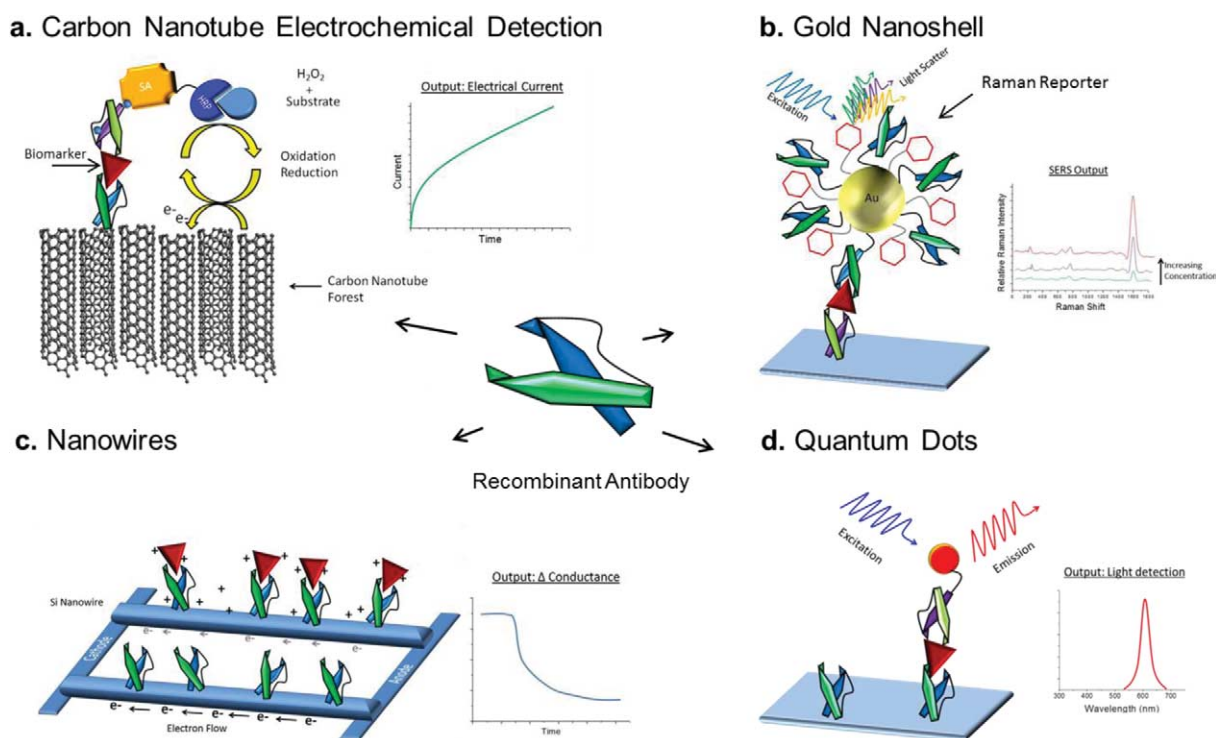


Fig. 4. Engineered antibodies coupled by nanotechnology for biosensing. Four different assay formats and readouts (insets) are shown here. (a) Carbon nanotubes in electrochemical detection: sandwich assay followed by oxidation of substrate by Horseradish peroxidase (HRP) results in an electrical current. (b) Gold nanoshell: changes in peak intensity in a Raman spectrum are detected when an antigen binds. (c) Nanowires: changes in current, upon analyte binding, are detected in a label-free manner. (d) Quantum dots: light output is detected at specific emission wavelengths.

the promise of simpler, quicker, and more sensitive assays. As nanostructures become cheaper and easier to fabricate, we anticipate the fields of biology and nanomaterials coming together to yield handheld portable devices for point-of-care diagnostics.

Carbon nanotubes

Carbon nanotubes (CNTs) (Fig. 4a) are hollow cylindrical nanostructures made up of carbons in a hexagonal construction, which have electrically and structurally interesting properties. They can be either single or multi-walled, with diameters between 0.3 and 100 nm (113). Carbon nanotubes can be utilized in two ways: one is through usage as an electrode in an oxidation-reduction electrochemical reaction, and the other as a Field Effect Transistor (FET), sensitive to changes in charge on the surface of the nanostructure.

First, we will discuss carbon nanotubes used in a system producing an electrochemical signal. This is assumed to be the most specific because of the requirement for dual antibody recognition of an antigen to generate a signal. An antigen can be detected in an immunosandwich assay (Fig. 6c), where the capture antibody is first immobilized to the surface of the CNT. The antigen is then added and allowed to bind to the capture antibody. The detection antibody, conjugated to

an HRP (Horseradish Peroxidase) enzyme, recognizes a secondary epitope of the antigen. Upon addition of a HRP substrate, an electrochemical redox reaction occurs to generate an electrical signal that is proportional to the amount of bound antigen (114).

Many current studies are using nanotube ‘forests’ (Fig. 6). These ‘forests’ are typically single-walled carbon nanotubes (SWCNT) arrayed in a vertical manner that are electrically conductive and allow for high-density antibody attachment and increased sensitivity. In one study (115), capture antibodies (Fig. 6b) are chemically attached to carbon nanotube forests (Fig. 6a) through primary amine coupling. In an example of bionanotechnology, Interleukin-6 (IL-6), a biomarker for Head and Neck Squamous Cell Carcinoma as well as for other cancers that cause inflammation, can be detected at lower limits of 30 pg/mL in serum. While patient blood analysis would be the eventual application for this nanotechnology, the ability to sensitively detect the tumor biomarker in serum demonstrates its relevance to potential usage in medical diagnostics. (Fetal calf serum is often used to simulate the assay conditions of a highly complex sample.) To be biologically relevant, the detection limit must be lowered at least 2-fold to the diseased target concentration of 19.5 pg/mL, and even lower for normal levels present at less than 6 pg/mL (116). To increase

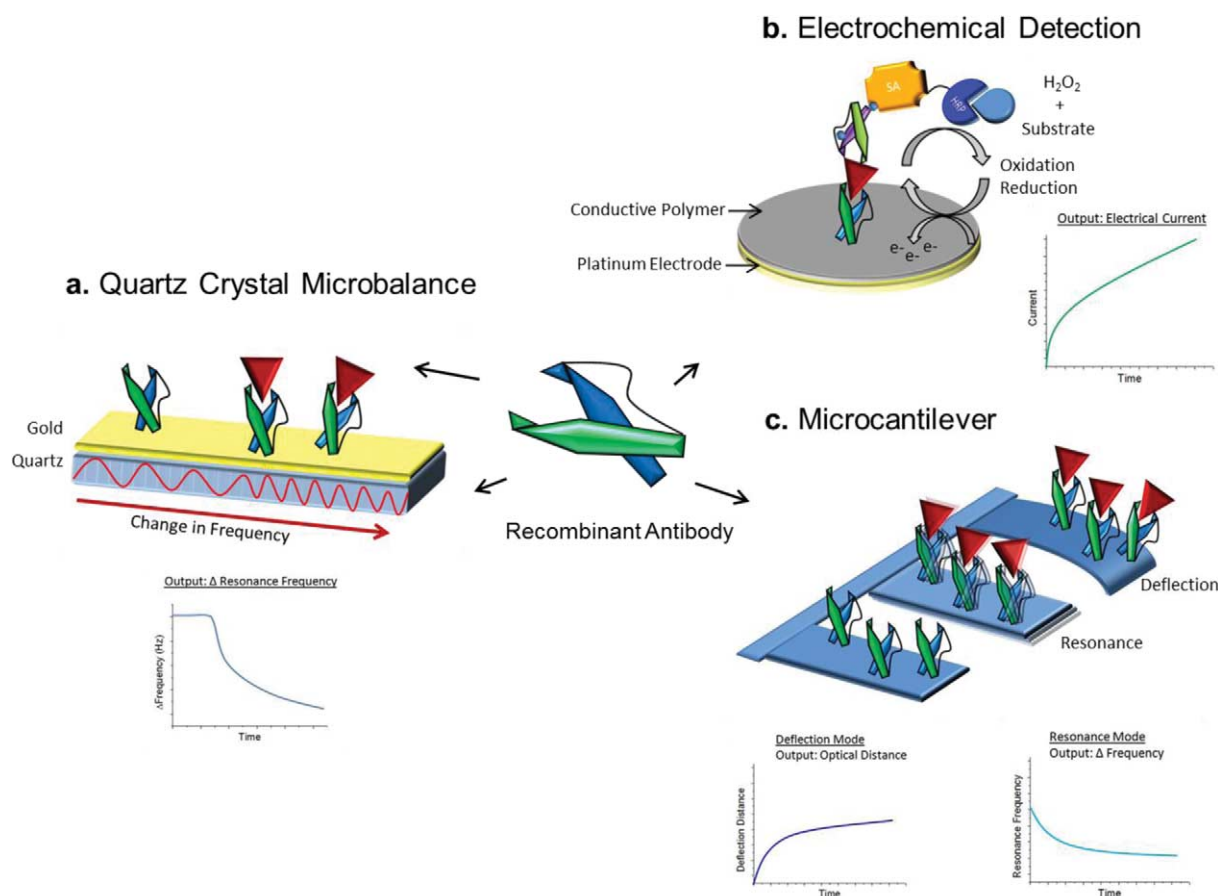


Fig. 5. Microscale technology biosensors. (a) Quartz crystal microbalance (QCM): changes in resonance frequency are detected in a label-free manner, upon analyte binding. (b) Electrochemical detection: platinum electrodes carry changes in current due to the oxidation–reduction reaction of HRP and its substrate. (c) Microcantilever: In Deflection mode, changes in bending of the cantilever are measured, whereas in Resonance mode, changes in resonance frequency are detected.

sensitivity, the same research group attached a multi-walled carbon nanotube (MWCNT), containing over 100 HRP molecules (Fig. 6d), to the detection antibody that provides amplification through current generation (Fig. 6e). With this enhanced system, the authors lowered the detection limit below healthy levels, with a 60-fold increase in sensitivity to 0.5 pg/mL, in fetal calf serum (117). This assay can be improved by multiplexing, so that a panel of biomarkers can be detected in a single sample, thereby increasing the test's diagnostic confidence. For diagnosing prostate cancer, four relevant biomarkers (PSA, PSMA, IL-6, and PF-4) can be tested with nanotube forests arrayed across four individual electrodes (118).

Carbon nanotubes can also be used as FETs (Fig. 7), where binding of an analyte to an anchored antibody causes a change in the environment near the surface of the nanotube, thereby altering the electrical conductance (119, 120). CNT-FET is expedient because only one antibody is required to capture the antigen and report a signal, as opposed to the dual antibody system described above. This was first shown in biomarker detection using an IgG

against the tumor marker, Carcinoembryonic antigen (CEA) (121). Later, engineered scFv antibodies were immobilized on Nickel nanoparticle coated nanotubes through the polyhistidine–Ni interaction. This resulted in a highly dense and orientation specific attachment and a subsequent 10-fold decrease in the detection limit of CEA (i.e. 10 ng/mL) (122).

In another study (123), an IgG antibody against the neurodegenerative disease and neuroendocrine tumor biomarker, Chromogranin A (CgA), is attached to a 2 nm thick single-walled carbon nanotube, through a 1-pyrenebutanoic acid succinimidyl ester linkage. Here, charge transfer from molecules adsorbing or binding to the nanotube surface causes a detectable change in resistivity. Because this biomarker protein is negatively charged at neutral pH, the binding of it near the nanotube causes an increase in electrical conductivity. The experimenters were able to detect 100 pM to 1 nM CgA, in a complex solution of fetal calf serum.

Finally, in a recent report implementing recombinant antibodies, a research group attached an anti-Osteopontin scFv antibody to a carbon nanotube FET

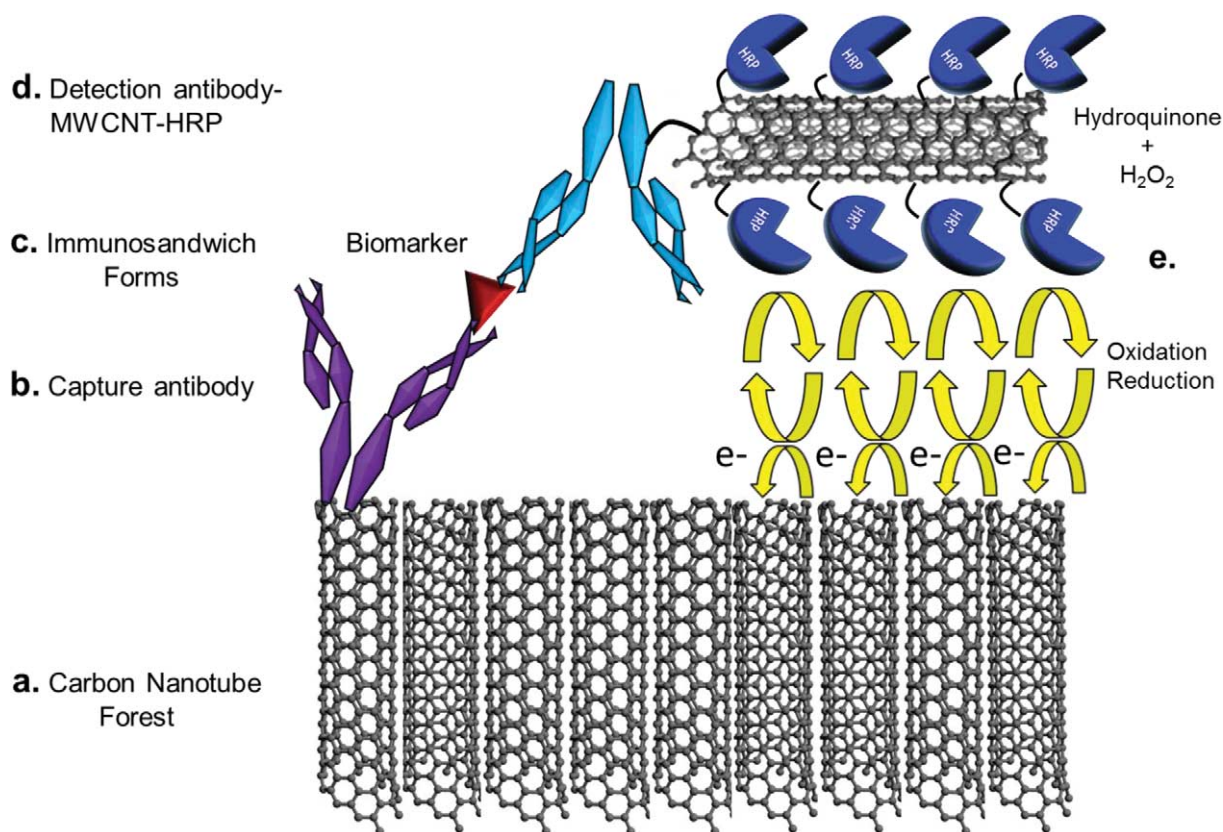


Fig. 6. Nanotube forest using multi-HRP carbon nanotube conjugated detection antibody for signal amplification. A capture antibody (b) is linked to a carbon nanotube ‘forest’ (a), through coupling by 1-ethyl-3-(3-dimethylaminopropyl) carbodiimide and *N*-hydroxysulfosuccinimide (EDC–NHSS) chemistry, to create an immunosensor. The sample containing the biomarker protein is then incubated with the immunosensor, and bound antigen is then detected with a second antibody (d) is attached to a multi-walled carbon nanotube in parallel with over 100 HRP molecules and incubated with the complex forming an immunosandwich (c). The sensor is then immersed in buffer with (e) hydroquinone and hydrogen peroxide where an oxidation of hydroquinone occurs. Upon application of voltage, an amperometric response is recorded.

(124). Osteopontin is a biomarker for tumor progression and an indicator of patient survival for many different cancers (125). Using the scFv-decorated carbon nanotube as a FET, the biomarker could be detected at physiologically relevant concentrations of 1 pg/mL.

Gold nanoshells, nanoparticles, and SERS

When light strikes a surface, the majority of photons are elastically scattered at the same energy of the incident photons (photons before striking the surface). However, a small number are scattered at a different energy. This inelastic scattering is known as Raman scattering (126–128). Fleischman et al., and others (129–131) discovered that pyridine, adsorbed to a roughened silver electrode surface, greatly enhanced the scattering effect. This was termed ‘Surface Enhanced Raman Scattering’ (SERS). Gold nanoshells (Fig. 4b) have been utilized as a scatter enhancing substrate for the attachment of antibodies and detection of binding events (132, 133). With inclusion of an attached molecule with a characteristic vibrational signal known as a Raman reporter, 10–100

different antibody–antigen interactions can potentially be monitored simultaneously, as the Raman vibrations of reporter molecules are narrow and do not overlap (134).

Using these principles, the tumor biomarker CEA was detected in an immunosandwich complex formed between a polyclonal antibody immobilized on a gold nanosphere and a monoclonal antibody attached to a magnetic particle. In this study (135), the gold nanosphere contained a Raman reporter, 4,4′-dipyridyl (DP), as well as the anti-CEA polyclonal IgG, which was attached through a primary amine linkage (Fig. 8a). A monoclonal antibody was attached to the magnetic particle in the same manner (Fig. 8b). Since both sets of antibodies are in solution, the constraint of a slow diffusion across a solid surface is eliminated. Upon mixing the CEA antigen with the antibody-linked particles, a concentration dependent shift of the Raman spectra peak intensity is observed (Fig. 8c and d). With the assay taking less than an hour to complete, a linear response can be detected in an antigen range of 1–100 pg/mL.

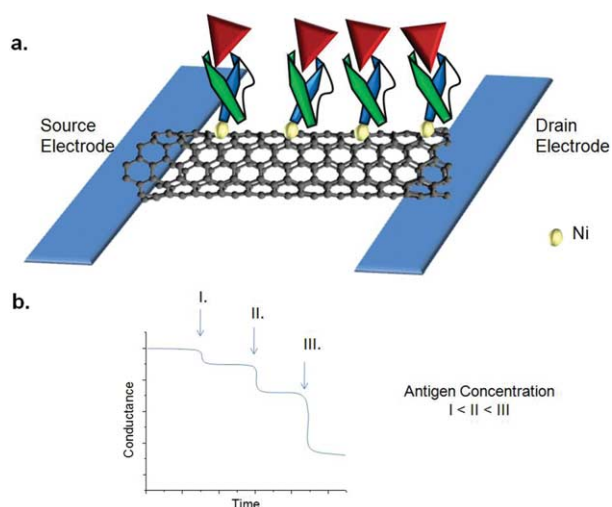


Fig. 7. Carbon nanotubes as a field effect transistor. (a) Single-walled carbon nanotubes (CNT) are connected, using photolithography, between source and drain electrodes. Nanotubes are then decorated with Nickel nanoparticles that have captured scFv molecules through the His₆ tag present at their C-termini. Upon addition of antigen to this nanofabricated structure, a change in the electrical conductance of the CNT is detected. (b) As antigen is added at increasing concentration (I–III), the conductance decreases over time.

In another report (136) showing the greatly enhanced sensitivity of nanostructures over traditional immunoassays, a monoclonal antibody was immobilized onto a gold electrode arrayed surface, while a polyclonal was attached to the nanosphere along with the Raman reporter Malachite Green isothiocyanate. Here, an attempt was made to detect a tumor growth biomarker, Angiogenin (ANG), as well as alpha-fetoprotein (AFP), a biomarker of hepatocellular carcinoma. When compared to standard ELISA, the SERS gold nanoshell immunoassay was reproducibly 1,000 times more sensitive in detecting the ANG at 0.1 pg/mL and 10,000 times more sensitive detecting the AFP at 1.0 pg/mL. This technique also provides a wider dynamic range than ELISA.

In a recent publication (137), recombinant antibodies of biomarkers for retinal injury have also been attached to nanoshells containing Raman reporters. Recombinant Fab antibodies selected against synthesized peptides of the photoreceptor cell specific calcium-ion channel protein, CACNA1F, were able to detect a response in 200 ng of total retinal lysate protein spotted on a nitrocellulose membrane, in a ‘half sandwich’ assay. The authors note that the CACNA1F protein composes less than 1% of the total protein and, therefore, the system is at a detection limit of ~2 ng.

In a final example showing the application in the study of living systems, Qian et al. (138) used pegylated gold nanoparticles decorated with scFvs against the tumor

biomarker epidermal growth factor receptor (EGFR), to detect the biomarker expressed on the surface of human carcinoma cells in culture. Going further, when injected into mice, the nanoparticle-linked scFvs were shown to accumulate at the site of a xenografted tumor (human head and neck squamous cell carcinoma overexpressing EGFR) and subsequently allowed SERS detection through the skin of the animal. These results demonstrate the low toxicity and compatibility of the gold nanoparticles in living systems, as well as the tumor targeting capacity of the scFv *in vivo*.

Nanowires

A nanowire (Fig. 4c) is a wire-like nanostructure that has a diameter in nanometers, but a length in micro to millimeters. These structures are considered one-dimensional because they have a length to width ratio of more than 1,000 and are confined in two dimensions (139). Nanowires can be made of conducting, insulating, or semi-conducting metals or metal alloys, but because these nanowires are so small in size, they have different physical properties than a wire of the same composition on the macro-scale (140). Silicon, for example, is generally used in the microchip industry as a semiconductor material. However, when silicon is grown into a nanowire, it can become an excellent conductor of electricity (141). Since the nanowires are so small in diameter, there are very few channels for an electron to travel as it moves through the material. The electron travels in a wave and has a quantum dimension known as the de Broglie wavelength of the electron. If a material has a dimension that is the same size or smaller than the de Broglie wavelength, then the electron cannot travel through and thus is confined to move through the other two dimensions. However, if two dimensions are confined, then the electron can travel in only one direction through the material. This confinement is what allows detection of changes in conductivity when charged molecules bind to the surface, altering the flow of electrons through the nanowire (142, 143).

Although nanowires have been used to detect various types of biological molecules, no one has yet implemented recombinant or engineered antibodies. However, it is easy to imagine the replacement of a traditional immunoglobulin with an antibody fragment, as we have seen previously in other nanostructured sensors. As a biosensor, Zheng and co-workers (144) use an array of nanowires to detect low concentrations of three cancer biomarker proteins. They do this by attaching monoclonal antibodies to electrically addressable nanowires and then recording any changes in conductance. They first coated silicon nanowires with Aldehyde Propyltrimethoxysilane (APTMS). Monoclonal antibodies raised against cancer biomarkers were applied to the surface by contact printing, where the aldehyde in the

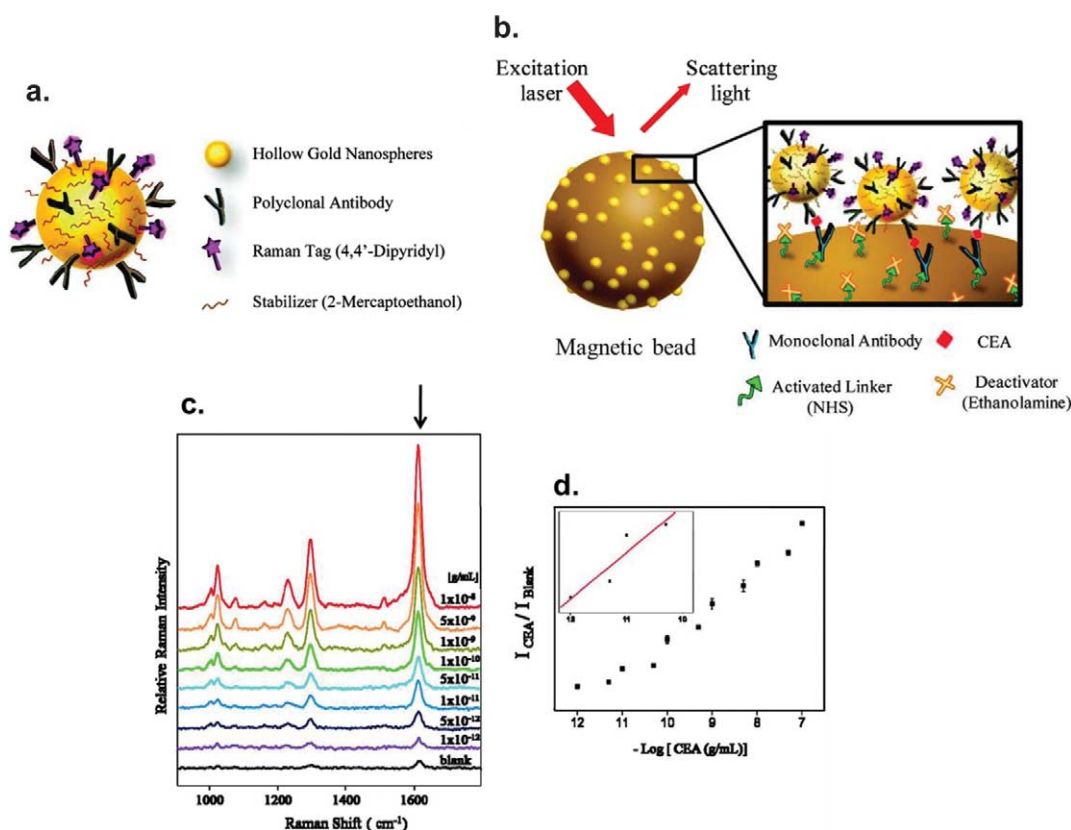


Fig. 8. SERS immunosandwich assay. (a) The gold nanoshell is functionalized with the anti-Carcinoembryonic antigen (CEA) polyclonal antibody along with the Raman reporter tag DP. (b) The larger magnetic bead is functionalized with a monoclonal antibody against the CEA antigen through a primary amine, by reacting them with *N*-hydroxysuccinimidyl (NHS). An immunosandwich forms when the polyclonal antibody from the nanoshell and the monoclonal antibody from the magnetic bead recognize the same CEA molecule simultaneously. When the complex is excited with a laser, a characteristic scattering spectrum is obtained. (c) Several surface enhanced Raman scattering (SERS) spectra are shown, with the wavelength along the *x*-axis and the relative intensity along the *y*-axis. The intensity shift is measured at the peak wavelength of 1612 cm^{-1} (arrow). The bottom black spectrum is the blank with no antigen, and, therefore, no immunosandwich forms. Moving from bottom to top shows the spectra at increasing concentrations of the CEA antigen and subsequent increases in immunosandwich formation that is detected by the increasing intensity at 1612 cm^{-1} . (d) The CEA concentration is plotted versus the intensity of the signal at 1612 cm^{-1} . The increase in intensity is concentration dependent.

Reprinted (adapted) with permission from Chon et al. (135). Copyright (2012) American Chemical Society.

APTMS forms bonds to free amines provided by lysine residues of the protein. This device, with less than 1 cm^2 area, was fabricated to include 200 nanowires. Potentially a different monoclonal antibody can be attached to each nanowire. A microfluidic channel running perpendicular to the array delivers sample to the nanowires. P-type or Positive-type (Boron Doped) silicon nanowires will give an increase in conductance when the antibody recognizes a negatively charged protein because a negative charge causes an accumulation of electrons. A positively charged protein binding event will give a decrease in conductance because it depletes the electrons, creating vacancies in the nanowire and therefore an increase in resistance.

To test their ability to detect proteins of disease, varied amounts of the cancer biomarker PSA are flowed over a single P-type nanowire. The change in conductance is

proportional to the log of the concentration of the negatively charged PSA and can be detected between an incredibly low 75 fg/mL ($\sim 2\text{ fM}$) and a physiological relevant high of 5 ng/mL ($\sim 160\text{ pM}$). The nanowire array device could also detect low concentrations of other cancer biomarkers, such as the tumor biomarker CEA and the colon cancer marker Mucin-1. The future success of such a device could be furthered with the use of many of the arrayed nanowires to perform assays on panels of biomarkers for a multitude of diseases using a single sample. With this in mind, the authors demonstrate that detection can be done in a multiplexed format amongst high concentrations of unrelated proteins in the form of human serum (144). As these devices continue to advance and become more robust sensing platforms, the application of recombinant antibodies will undoubtedly emerge.

Quantum dots

Semiconductor quantum dots (QDs) (Fig. 4d) have emerged as popular nanostructures for imaging, tracking, and sensing biomarkers in tissues and within cells (145). They are semiconducting nanocrystals with diameters of 1–10 nm, composed of a core and an outer shell layer where a CdSe core and an outer layer of ZnS form one of the most popular such QDs. QDs display unique properties because of the phenomenon termed ‘quantum confinement’. When the particle size has a radius smaller than the electron orbit of the semiconductor, confinement occurs in three dimensions. This causes a shift to a higher energy state, releasing a higher energy light emission upon absorption of a photon (reviewed in (146, 147)). The size of the crystal dictates the emission peak and can be tailored to a wide range of wavelengths with narrow emission peaks. This gives QDs an advantage over traditional fluorophores by permitting increased options for multiplexing (148). More importantly, QDs also are more photostable and more resistant to photobleaching than most fluorophores (149). Since QDs have been reported to have difficulty crossing membranes (150), many studies have utilized QDs to probe cell surface targets of cell and tissues (151). However, through the use of peptide translocation domains attached to QDs, internalization into the cell occurs readily (152).

In one interesting study involving these technologies, researchers attached dimers of scFvs, called cys-diabodies, to pegylated QDs. The cys-diabody selected against the breast cancer cell surface antigen HER2 was used with a CdSe/ZnS QD emitting a peak wavelength at 655 nm. A second diabody against the prostate cancer antigen PSCA was coupled to a QD emitting at 800 nm. When combined together, it is now possible to image the two surface antigens simultaneously on cultured tumor cells expressing both PSCA and HER2. (150). An even smaller engineered antibody, the single domain antibody (sdAb)(Fig. 2d) of camelids (36) was utilized in another study. These are heavy chain single domain antibodies with a size half that of an scFv, and dissociation constants in the mid pM to high nM range (153). The sdAbs were engineered to complex with a CdSe/ZnS QD to detect the tumor marker EGFR in breast cancer cells (154).

Recent experiments have been able to identify tumors in whole organism body scans using injected scFv linked QDs (155). An anti-HER2 scFv conjugated to a QD was injected into immunodeficient mice carrying a xenografted human breast cancer. The technique, Diffuse Fluorescence Tomography (DFT), was then used to image the entire mouse (Fig. 9). The scFv specifically targeted the cell surface antigens in the tumor and the brightness of QDs provided a contrasting agent for visualization of the cancer through the skin of the animal using tomography.

Quartz crystal microbalance sensing

Quartz crystal microbalance (QCM) (Fig. 5a) sensing is based on the direct linear relationship between mass accumulated on the surface and a change in the resonance frequency of a piezoelectric crystal, as first described by Sauerbrey (156). Since resonance frequency depends on mass, data recording is performed in real-time, where multiple binding events can be measured in series. Recently, QCMs have been used for detection of biomarkers in a label-free manner. Uludag et al. (157) utilized SAMs to attach monoclonal IgG antibodies, generated against PSA, to the surface of the crystal. They could detect PSA down to 18.8 ng/mL in phosphate buffered saline (PBS), but found that using a second detection antibody brought the detection limit to 4.7 ng/mL. The second antibody created an immunosandwich, which boosted the change in resonance frequency because of the increase in accumulated mass. The sandwich was required when probing a complex solution with high concentrations of proteins, like human serum, to achieve sensitive detection (i.e. 9.4 ng/mL) of PSA. Further, modification of the detection antibody with 40 nm gold nanoparticles again increased the mass, and permitted a 30-fold increase in sensitivity down to 0.29 ng/mL. This sensitive detection in the complex sample shows the relevance of the technique in a more plausible clinical scenario (157).

Shen et al. (158) first showed the possibility of using scFv engineered antibodies, coupled to a gold-coated QCM, to detect a protein in solution. By replacing two amino acid residues with histidines in the linker region of the antibody, they took advantage of the strong and orientation specific interaction that histidine is known to have with gold (159). As a proof of concept, they used a scFv selected against rabbit IgG to detect 350 ng/mL of the antibody in PBS. The same group later translated their method from conceptual to a more medically relevant application by detecting the breast cancer biomarker Cytochrome P450 1B1 (CYP1B1). Here they synthesized peptides 13–14 amino acids in length, which correspond to a region of the CYP1B1 that distinguishes it from other closely related members of the Cytochrome P450 family. ScFv antibodies were then generated from a phage-display library selection against these peptides. These recombinant antibodies also recognize the peptide when it is part of the full-length biomarker. The scFvs were attached to the gold-coated crystal through a biotin–neutravidin linkage, allowing for a high-density packing of the antibody (Fig. 10a). Using cancer cell lysates and breast cancer microsomes, the group was able to detect CYP1B1 down to 130 ng/mL (2.2 nM) *via* the scFv-QCM biosensor (Fig. 10b and c). Finally, they used the QCM biosensor to quantify the protein biomarker in various lysates of cancerous cell lines versus healthy cell lysates,

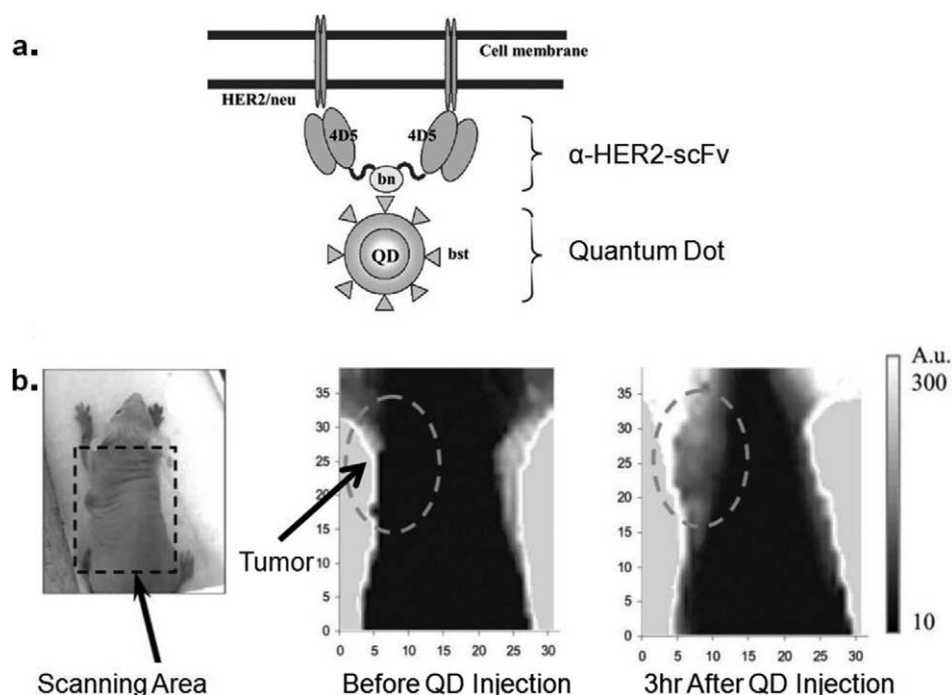


Fig. 9. *In vivo* imaging using Quantum Dots (QD) that are conjugated to scFvs. (a) Two anti-HER2-scFvs are conjugated to a 705 nm emitting QD, using the Barnase(bn)–Barstar(bst) system, which is similar in binding strength to biotin–streptavidin. The antibody targets the HER2 (Erb2-Human Epidermal growth factor Receptor 2). (b) A mouse bearing a human breast cancer tumor is imaged using diffuse fluorescence tomography, before and after intravenous injection of 150 pM of scFv-QD conjugates. Signal increase was observed from 0.5 to 9 h after injection. Reproduced with permission from Balalaeva et al., 2012 (155).

demonstrating the diagnostic and disease progression monitoring capabilities of their system (160).

Electrochemical detection

Electrochemistry (Fig. 5b) has been an attractive analytical technique because of the sensitive and wide dynamic range of detection, the ability to adapt into many miniature formats, and in large part to the success of the blood glucose meter, which comprises 85% of biosensor sales (161). These devices either sense a change in voltage (potentiometric) or a change in current (amperometric) due to binding of antigens within the biosensor. Potentiometric devices sense the production of an ion from a reaction between an enzyme and a substrate, while amperometric devices detect changes in current due to an oxidation–reduction of an electrochemical reaction. In the case of an immunoassay, usually a two-antibody sandwich recognition system is required. A capture antibody is immobilized to a transducer such as an electrode, conductive polymer, carbon nanotube, or gold nanoshell. The sample containing the antigen is then applied. A second detection antibody specific for a different epitope of the same antigen carries an enzyme that provides an electrical signal upon addition of a substrate (162, 163).

In a commercial application of an electrochemical detection assay, CombiMatrix Corporation (now CustomArray Incorporated), developed a multiplexed sand-

wich immunoassay that can be performed on thousands of individually addressable platinum electrodes that fit in a square centimeter of a complementary metal oxide semiconductor (CMOS) microchip (164). Antibodies can be specifically attached to a desired location by first synthesizing a unique DNA oligonucleotide directly on an electrode. Hybridization to a unique complementary oligonucleotide conjugated to the capture antibody, immobilizes the antibody to the electrode. After antigen addition, a biotinylated detection antibody is incubated followed by a streptavidin–HRP (SA–HRP). With the addition of an HRP substrate, an oxidation–reduction reaction occurs, creating an electron flow detected by the electrode below the sandwich complex. Using this scheme, the liver inflammation biomarker, α -1-acid glycoprotein (AGP), was detected at a lower detection limit of 5 pg/mL, in a sample volume of 50 μ L (161). While this ability for multiplexing and immobilizing of antibody in a parallel manner by a DNA barcode system is advantageous, which has also been used in other platforms in what is known as DNA-encoded antibody libraries (DEAL) (165), the sandwich ELISA scheme requires multiple antibodies for each analyte, followed by an amplification step before reading.

Alternatively, the assay could be designed to utilize only one antibody and no amplification step. In a recent study (162), a sensitive, label-free electrochemical biosensor was

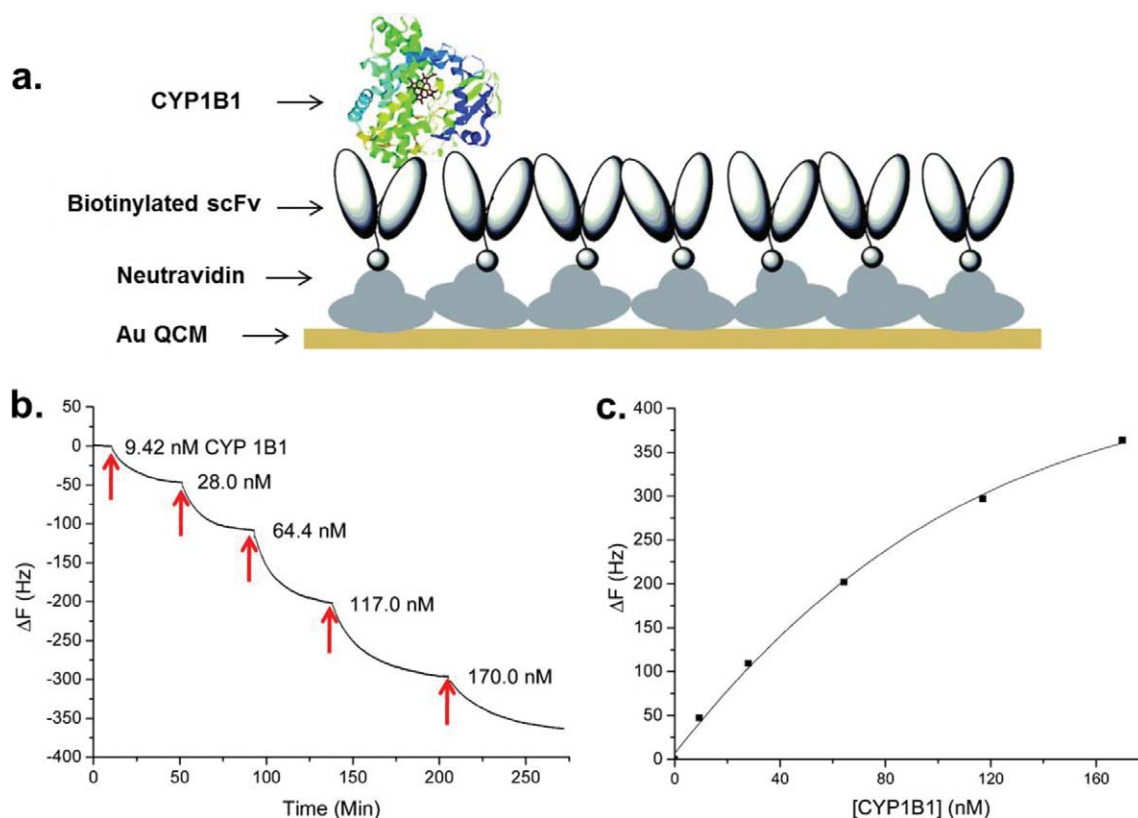


Fig. 10. Detection of Cytochrome P450 1B1 using scFvs on QCM. (a) NeutrAvidin®, an engineered version of avidin, is immobilized on a gold-coated quartz surface (QCM). Chemically biotinylated scFv antibody against CYP1B1 was allowed to tightly pack on the surface. (Orientation is more disordered than as shown.) (b) A dose response is shown with the addition of CYP1B1 (ribbon representation of its three-dimensional structure) to the antibody-immobilized surface. Arrows show addition of different concentrations of antigen over time: the resulting change in frequency can be observed over time, where the greater the concentration of antigen, the greater the change in frequency. (c) The calibration curve is plotted with the change in frequency against concentration of antigen. The curve is concentration dependent.

Reprinted (adapted) with permission from Shen et al. (160). Copyright (2012) American Chemical Society.

developed by first incorporating scFvs onto an electrically conductive polymer, polypyrrole, deposited on a gold electrode. The differential pulse voltammetry (DPV) of electrodes coated with antibody is then recorded and used as a baseline reading. Subsequent binding of an antigen causes a reduction in electrical current from baseline by blocking charge transport of ions to the surface and therefore inhibiting the electron transfer. The decrease in current is proportional to the amount bound to the antibody. Here, they report a linear, concentration dependent response in current from antigen binding at concentrations from 1 pg/mL down to 100 ng/mL.

Microcantilevers

Microcantilevers (Fig. 5c) are micrometer thin projections that are sensitive to changes in surface mass. Immobilization of antibodies to the cantilever surface allows one to probe sample mixtures in two modes. The Resonance mode detects the mechanical bending and, therefore, a change in resonance frequency upon accumulation of

material on the cantilever (166). In Deflection mode, the antibody is deposited on one side of the cantilever and upon binding of the analyte, a mechanical stress and physical bending of the cantilever is measured. To perform the deflection measurements, there are optical methods that monitor the interference in a reference laser by the reflection of a laser focused on the surface of a cantilever. In addition, there are piezoresistive methods that measure the change in resistance upon deflection, and there are also microelectronic methods that measure changes in capacitance. In the Resonance mode, the changes in the frequency of natural oscillations of the microcantilever can be measured to detect antibody–antigen recognition events. The most common way to do this is through the use of piezoelectric materials that convert the resonance frequency to an electrical signal whereby changes can be sensitively detected. A more sensitive method is to integrate sealed microfluidic channels into the cantilevers where the sample is passed through. Deposited antibody in the channels

captures the analyte resulting in a detectable change in frequency (167).

In the very first use of a microcantilever device for the detection of a biomarker, Wu et al. (168) immobilized polyclonal anti-PSA antibodies on gold-coated silicon nitride cantilevers. The method here was to attach the antibodies to one side of the cantilever and record the deflection caused by antibody–antigen binding. In a background of human plasma, the device could detect PSA at concentrations between 60 and 200 pg/mL. More recently, using mechanical resonance frequency shifts of a piezoelectric cantilever coated with antibody, another

group was able to detect PSA at concentrations as low as 10 pg/mL (169).

The first application of scFvs to microcantilevers involved the functionalization of anti-peptide scFvs on single-sided, gold-coated silicon (26). With the capability to engineer the antibody fragment through simple molecular biology techniques, a cysteine amino acid was added to the C-terminus for directing the attachment of the antibody fragment to the gold-coated cantilever. By monitoring the deflections of the cantilever in solution for 30–60 min, the device was able to detect the peptide fragment at 20 ng/mL (i.e. 1 nM). Very recently,

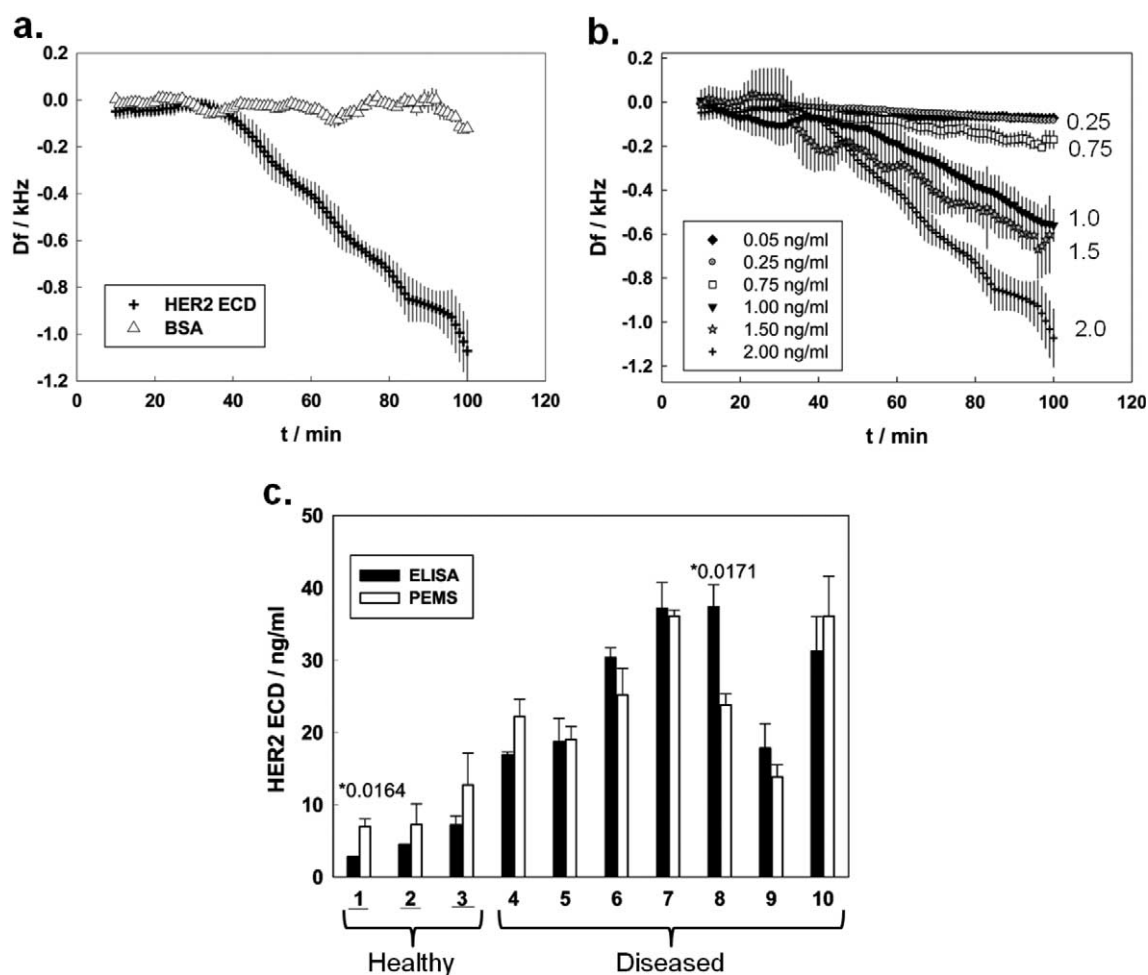


Fig. 11. Detection of breast cancer biomarker using piezoelectric microbalance. The anti-HER2 antibody (trastuzumab, trade name ‘Herceptin’) is first functionalized to a Piezoelectric Microbalance Sensor (PEMS) through an amine-sulphydryl linkage, and the sensor is then placed in a flow cell. (a) Serum-spiked recombinant HER2–Extracellular Domain (ECD) is administered to the flow cell, and a change in vibrational frequency (kHz) is shown. Addition of the negative control protein, Bovine Serum Albumin (BSA), shows no change in frequency. (b) Additions of increasing concentration of the HER2–ECD give increasing changes in frequency. The sensitivity is adequate to detect healthy levels in the low nanogram per milliliter range. (c) PEMS detecting concentrations of HER2 in serum from confirmed breast cancer patients is shown in samples 4 through 10, and is also compared to ELISA results in the adjacent bar. Patient samples 1–3 are healthy, negative controls. In general, the PEMS results are consistent with the ELISA data, with the exception of patient #1 and #8 that show significant differences between the two. This was attributed to the prototype apparatus, but the difference in signals between healthy vs. diseased is apparent. Reprinted (adapted) with permission from Adams et al. (170). Copyright (2012) American Chemical Society.

a group functionalized and attached the Fab, trastuzumab (Herceptin®), to a piezoelectric cantilever, in an attempt to detect the breast cancer marker HER2 (170). In spiked human serum (Fig. 11a and b), detection limits of the trastuzumab sensor were shown to be less than 2 ng/mL, which is within the normal range of concentration of HER2 present in the serum of healthy individuals, and, therefore, is well below the threshold level of disease. In a stunning clinical application of the instrument, the authors used serum from confirmed breast cancer patients to show the assay is capable of distinguishing between healthy controls and diseased patients (Fig. 11c). Through the correct identification of patients with tumors, future diagnosis of breast cancer by this assay looks promising.

Photonic crystal binding assays

Although photonic crystals are relatively new to the arena of nanostructured biosensors, they are worth mentioning briefly (171). These biosensors are label-free, high throughput, and detect protein binding to a nanostructured surface in real-time (172). The photonic crystals are composed of a layer of low refractive index material and a layer of high refractive index dielectric material. This optical resonator allows most wavelengths from a light source to pass, but reflects a narrow range of wavelengths that are collected by a spectrometer and recorded as the peak wavelength value. As proteins accumulate on the surface or bind to molecules deposited on the surface, the wavelengths allowed to pass begin to change, which causes the reflected light to increase in wavelength. This change in the peak wavelength is directly proportional to the adsorbed mass and, therefore, can quantify antibody-antigen binding events. Recently, these principles were used to enhance fluorescence signals by 1,000-fold or more from traditional fluorophore conjugated antibodies in protein microarrays. Eighteen cancer biomarkers were detected in the array with lower limits nearing the single pg/mL range (173). As the sensitivity of these biosensors improves, the potential for its application in medical diagnostics will become more apparent and practical.

Conclusion

Employing the powerful technology of phage-displayed library selection to obtain specific antibodies for the detection of biomarkers, combined with the extremely small size, multiplexing ability, and high sensitivity of nanostructures, one can imagine the impact of on the spot diagnosis of disease and injury, on public health. These antibody-coupled nanodevices have many advantages over traditional immunoassays of ELISA or Western blotting. The small size of the devices, and the ability to integrate nanomaterials and microelectronics into microfluidic sample delivery systems, greatly simpli-

fies the assay, making it convenient, sensitive, robust, and low-cost. Furthermore, many of the laborious and time consuming steps of traditional immunoassays can be replaced with a nanodevice, which would require a minimum amount of sample preparation and processing time, thereby yielding a rapid, yet accurate, result. Many devices also provide for multiplexing detection of panels of biomarkers for a more confident diagnosis. Finally, the unique physical properties like quantum confinement and Raman scattering allow for label-free, real-time sensing of the presence of molecules and also, in other cases, as a spatial locator of molecules within cells or tissues.

Emerging recently is the first of the personalized ‘omics’ (proteomics, genomics, and metabolomics) studies that can track thousands of biochemical changes in the body to an extent where onset of disease can actually be reversed (174). We envision that one day this powerful diagnostic will be in the hands of the general public, where nanostructured immunoassays will be tailored for the individual based on their sequenced genome, their occupation, and their lifestyle. This will allow for the earliest detection of malignant tumors, onset of inherited diseases, or injury to internal organs, and subsequently allow for proper treatment. We can also speculate further to include the detection and identification of environmental biological agents, bacterially contaminated food, tainted water, or polluted air, available for immediate analysis in a sensitive, easy to use, hand-held instrument.

Acknowledgements

We would like to thank Drs. Mitra Dutta (Department of Electrical and Computer Engineering, UIC), David T. Eddington (Department of Bioengineering, UIC), and members of the laboratory for their editorial help. Salary support was provided in part by US Air Force grant # FA 7014-07-C-0047.

Conflict of interest and funding

There is no conflict of interest in the present study for any of the authors.

References

1. Blonder J, Issaq HJ, Veenstra TD. Proteomic biomarker discovery: its more than just mass spectrometry. *Electrophoresis* 2011; 32: 1541–8. Available from: <http://onlinelibrary.wiley.com/doi/10.1002/elps.201000585/full>
2. Simpson KL, Whetton AD, Dive C. Quantitative mass spectrometry-based techniques for clinical use: biomarker identification and quantification. *J Chromatogr B Analyt Technol Biomed Life Sci* 2009; 877: 1240–9. Available from: <http://www.sciencedirect.com/science/article/pii/S1570023208008453>
3. Hunt DF, Yates JR III, Shabanowitz J, Winston S, Hauer CR. Protein sequencing by tandem mass spectrometry. *Proc Natl Acad Sci USA* 1986; 83: 6233–7. Available from: <http://www.pnas.org/content/83/17/6233.short>

4. Rifai N, Gillette MA, Carr SA. Protein biomarker discovery and validation: the long and uncertain path to clinical utility. *Nat Biotechnol* 2006; 24: 971–83. Available from: <http://www.nature.com/nbt/journal/v24/n8/full/nbt1235.html>
5. Braunstein GD, Rasor J, Danzer H, Adler D, Wade ME. Serum human chorionic gonadotropin levels throughout normal pregnancy. *Am J Obstet Gynecol* 1976; 126: 678–81. Available from: <http://www.ncbi.nlm.nih.gov/pubmed/984142>
6. Waller DK, Lustig LS, Smith AH, Hook EB. Alpha-fetoprotein: a biomarker for pregnancy outcome. *Epidemiology* 1993; 4: 471–6. Available from: http://journals.lww.com/epidem/Abstract/1993/09000/Alpha_Fetoprotein__A_Biomarker_for_Pregnancy.14.aspx
7. Thygesen K, Alpert JS, White HD. Universal definition of myocardial infarction. *J Am Coll Cardiol* 2007; 50: 2173–95. Available from: <http://www.sciencedirect.com/science/article/pii/S0735109707029579>
8. Pineda JA, Lewis SB, Valadka AB, Papa L, Hannay HJ, Heaton SC, et al. Clinical significance of alphaII-spectrin breakdown products in cerebrospinal fluid after severe traumatic brain injury. *J Neurotrauma* 2007; 24: 354–66. Available from: <http://online.liebertpub.com/doi/abs/10.1089/neu.2006.003789>
9. Banyan Biomarker Immunoassays. Available from: <http://banyanbio.com> [cited 15 December 2011].
10. Gold P, Freedman SO. Demonstration of tumor-specific antigens in human colonic carcinomata by immunological tolerance and absorption techniques. *J Exp Med* 1965; 121: 439–62. Available from: <http://jem.rupress.org/content/121/3/439.abstract>
11. Bast RC Jr., Feeney M, Lazarus H, Nadler LM, Colvin RB, Knapp RC, et al. Reactivity of a monoclonal antibody with human ovarian carcinoma. *J Clin Invest* 1981; 68: 1331–7. Available from: <http://www.jci.org/articles/view/110380>
12. Stamey TA, Yang N, Hay AR, McNeal JE, Freiha FS, Redwine E, et al. Prostate-specific antigen as a serum marker for adenocarcinoma of the prostate. *N Engl J Med* 1987; 317: 909–16. Available from: <http://www.nejm.org/doi/full/10.1056/NEJM198710083171501>
13. Pane F, Frigeri F, Sindona M, Luciano L, Ferrara F, Cimino R, et al. Neutrophilic-chronic myeloid leukemia: a distinct disease with a specific molecular marker (BCR/ABL with C3/A2 junction). *Blood* 1996; 88: 2410–4. Available from: <http://bloodjournal.hematologylibrary.org/content/88/7/2410.long>
14. Ross JS, Fletcher JA, Linette GP, Stec J, Clark E, Ayers M, et al. The HER-2/neu gene and protein in breast cancer 2003: biomarker and target of therapy. *Oncologist* 2003; 8: 307–25. Available from: <http://theoncologist.alphamedpress.org/content/8/4/307.full>
15. Kohler G, Milstein C. Continuous cultures of fused cells secreting antibody of predefined specificity. *Nature* 1975; 256: 495–7. Available from: <http://www.nature.com/nature/journal/v256/n5517/pdf/256495a0.pdf>
16. Kotlan B, Glassy MC. Antibody phage display: overview of a powerful technology that has quickly translated to the clinic. *Methods Mol Biol* 2009; 562: 1–15. Available from: <http://www.springerlink.com/content/j247u08447122q23/#section=91327&page=1>
17. Clamp M, Fry B, Kamal M, Xie X, Cuff J, Lin MF, et al. Distinguishing protein-coding and noncoding genes in the human genome. *Proc Natl Acad Sci USA* 2007; 104: 19428–33. Available from: <http://www.pnas.org/content/104/49/19428.long>
18. Lo AS, Zhu Q, Marasco WA. Intracellular antibodies (intrabodies) and their therapeutic potential. *Handb Exp Pharmacol* 2008; 181: 343–73. Available from: <http://www.springerlink.com/content/j67v48494178505k/>
19. Cardinale A, Biocca S. The potential of intracellular antibodies for therapeutic targeting of protein-misfolding diseases. *Trends Mol Med* 2008; 14: 373–80. Available from: <http://www.sciencedirect.com/science/article/pii/S1471491408001500>
20. Boder ET, Midelfort KS, Wittrup KD. Directed evolution of antibody fragments with monovalent femtomolar antigen-binding affinity. *Proc Natl Acad Sci USA* 2000; 97: 10701–5. Available from: <http://www.pnas.org/content/97/20/10701.long>
21. Hanes J, Schaffitzel C, Knappik A, Pluckthun A. Picomolar affinity antibodies from a fully synthetic naive library selected and evolved by ribosome display. *Nat Biotechnol* 2000; 18: 1287–92. Available from: <http://www.nature.com/doifinder/10.1038/82407>
22. Abler LL, Sheets MD. Expression of scFv antibodies in *Xenopus* embryos to disrupt protein function: implications for large-scale evaluation of the embryonic proteome. *Genesis* 2003; 35: 107–13. Available from: <http://onlinelibrary.wiley.com/doi/10.1002/gene.10171/abstract>
23. Gulyani A, Allan R, Wu J, Gremyachinskiy D, Lewis S, Dewar B, et al. A Src family biosensor based on an engineered scaffold enables sensitive quantitation. *Nat Chem Biol* 2011; 7: 437–44. Available from: <http://www.nature.com/nchembio/journal/v7/n7/full/nchembio.585.html>
24. Liu CC, Mack AV, Tsao ML, Mills JH, Lee HS, Choe H, et al. Protein evolution with an expanded genetic code. *Proc Natl Acad Sci USA* 2008; 105: 17688–93. Available from: <http://www.pnas.org/content/105/46/17688.long>
25. Athavankar S, Peterson BR. Control of gene expression with small molecules: biotin-mediated acylation of targeted lysine residues in recombinant yeast. *Chem Biol* 2003; 10: 1245–53. Available from: <http://www.sciencedirect.com/science/article/pii/S1074552103002527>
26. Hegner M, Backmann N, Zahnd C, Huber F, Bietsch A, Pluckthun A, et al. A label-free immunosensor array using single-chain antibody fragments. *Proc Natl Acad Sci USA* 2005; 102: 14587–92. Available from: <http://www.pnas.org/content/102/41/14587.abstract>
27. Fredriksson S, Gullberg M, Jarvius J, Olsson C, Pietras K, Gustafsdottir SM, et al. Protein detection using proximity-dependent DNA ligation assays. *Nat Biotechnol* 2002; 20: 473–7. Available from: <http://www.nature.com/nbt/journal/v20/n5/full/nbt0502-473.html>
28. Soderberg O, Gullberg M, Jarvius M, Ridderstrale K, Leuchowius KJ, Jarvius J, et al. Direct observation of individual endogenous protein complexes in situ by proximity ligation. *Nat Methods* 2006; 3: 995–1000. Available from: <http://www.nature.com/nmeth/journal/v3/n12/full/nmeth947.html>
29. Schallmeiner E, Oksanen E, Ericsson O, Spangberg L, Eriksson S, Stenman UH, et al. Sensitive protein detection via triple-binder proximity ligation assays. *Nat Methods* 2007; 4: 135–7. Available from: <http://www.nature.com/nmeth/journal/v4/n2/full/nmeth974.html>
30. Gullberg M, Gustafsdottir SM, Schallmeiner E, Jarvius J, Bjarnegard M, Betsholtz C, et al. Cytokine detection by antibody-based proximity ligation. *Proc Natl Acad Sci USA* 2004; 101: 8420–4. Available from: <http://www.pnas.org/content/101/22/8420.long>
31. Adams GP, Schier R, McCall AM, Simmons HH, Horak EM, Alpaugh RK, et al. High affinity restricts the localization and tumor penetration of single-chain fv antibody molecules. *Cancer Res* 2001; 61: 4750–5. Available from: <http://cancerres.aacrjournals.org/content/61/12/4750.long>
32. Bird RE, Hardman KD, Jacobson JW, Johnson S, Kaufman BM, Lee SM, et al. Single-chain antigen-binding

- proteins. *Science* 1988; 242: 423–6. Available from: <http://www.sciencemag.org/content/242/4877/423.long>
33. Huston JS, Levinson D, Mudgett-Hunter M, Tai MS, Novotny J, Margolies MN, et al. Protein engineering of antibody binding sites: recovery of specific activity in an anti-digoxin single-chain Fv analogue produced in *Escherichia coli*. *Proc Natl Acad Sci USA* 1988; 85: 5879–83. Available from: <http://www.pnas.org/content/85/16/5879.long>
 34. Hanes J, Jermutus L, Weber-Bornhauser S, Bosshard HR, Pluckthun A. Ribosome display efficiently selects and evolves high-affinity antibodies in vitro from immune libraries. *Proc Natl Acad Sci USA* 1998; 95: 14130–35. Available from: <http://www.pnas.org/content/95/24/14130.abstract>
 35. Rader C. Overview on concepts and applications of Fab antibody fragments. *Curr Protoc Protein Sci* 2009; Chapter 6: Unit 6.9. Available from: <http://onlinelibrary.wiley.com/doi/10.1002/0471140864.ps0609s55/abstract>
 36. Hamers-Casterman C, Atarhouch T, Muyldermans S, Robinson G, Hamers C, Songa EB, et al. Naturally occurring antibodies devoid of light chains. *Nature* 1993; 363: 446–8. Available from: <http://www.nature.com/nature/journal/v363/n6428/abs/363446a0.html>
 37. Saerens D, Ghassabeh GH, Muyldermans S. Single-domain antibodies as building blocks for novel therapeutics. *Curr Opin Pharmacol* 2008; 8: 600–8. Available from: <http://www.sciencedirect.com/science/article/pii/S1471489208000957>
 38. Koide A, Bailey CW, Huang X, Koide S. The fibronectin type III domain as a scaffold for novel binding proteins. *J Mol Biol* 1998; 284: 1141–51. Available from: <http://www.sciencedirect.com/science/article/pii/S0022283698922380>
 39. Forrer P, Stumpp MT, Binz HK, Pluckthun A. A novel strategy to design binding molecules harnessing the modular nature of repeat proteins. *FEBS Lett* 2003; 539: 2–6. Available from: <http://www.sciencedirect.com/science/article/pii/S0014579303001777>
 40. Binz HK, Stumpp MT, Forrer P, Amstutz P, Pluckthun A. Designing repeat proteins: well-expressed, soluble and stable proteins from combinatorial libraries of consensus ankyrin repeat proteins. *J Mol Biol* 2003; 332: 489–503. Available from: <http://www.sciencedirect.com/science/article/pii/S0022283603008969>
 41. Nord K, Gunneriusson E, Ringdahl J, Stahl S, Uhlen M, Nygren PA. Binding proteins selected from combinatorial libraries of an alpha-helical bacterial receptor domain. *Nat Biotechnol* 1997; 15: 772–7. Available from: <http://www.nature.com/nbt/journal/v15/n8/full/nbt0897-772.html>
 42. Huang R, Fang P, Kay BK. Isolation of monobodies that bind specifically to the SH3 domain of the Fyn tyrosine protein kinase. *New Biotechnol* 2012; 29: 526–533. Available from: <http://www.sciencedirect.com/science/article/pii/S1871678411002640>
 43. Boersma YL, Pluckthun A. DARPins and other repeat protein scaffolds: advances in engineering and applications. *Curr Opin Biotechnol* 2011; 22: 849–57. Available from: <http://www.sciencedirect.com/science/article/pii/S095816691100615X>
 44. Boersma YL, Chao G, Steiner D, Wittrup KD, Pluckthun A. Bispecific designed ankyrin repeat proteins (DARPins) targeting epidermal growth factor receptor inhibit A431 cell proliferation and receptor recycling. *J Biol Chem* 2011; 286: 41273–85. Available from: <http://www.jbc.org/content/286/48/41273.long>
 45. Lofblom J, Feldwisch J, Tolmachev V, Carlsson J, Stahl S, Frejd FY. Affibody molecules: engineered proteins for therapeutic, diagnostic and biotechnological applications. *FEBS Lett* 2010; 584: 2670–80. Available from: <http://www.sciencedirect.com/science/article/pii/S001457931000284X>
 46. Oliphant AR, Brandl CJ, Struhl K. Defining the sequence specificity of DNA-binding proteins by selecting binding-sites from random-sequence oligonucleotides – analysis of yeast GCN4 protein. *Mol Cell Biol* 1989; 9: 2944–9. Available from: <http://mcb.asm.org/content/9/7/2944.long>
 47. Tuerk C, Gold L. Systematic evolution of ligands by exponential enrichment – RNA ligands to bacteriophage-T4 DNA-polymerase. *Science* 1990; 249: 505–10. Available from: <http://www.jstor.org/stable/view/2874490>
 48. Ellington AD, Szostak JW. In vitro selection of RNA molecules that bind specific ligands. *Nature* 1990; 346: 818–22. Available from: <http://www.nature.com/nature/journal/v346/n6287/abs/346818a0.html>
 49. Yonezawa M, Doi N, Kawahashi Y, Higashinakagawa T, Yanagawa H. DNA display for in vitro selection of diverse peptide libraries. *Nucleic Acids Res* 2003; 31: e118. Available from: <http://nar.oxfordjournals.org/content/31/19/e118.long>
 50. Roberts RW, Szostak JW. RNA-peptide fusions for the in vitro selection of peptides and proteins. *Proc Natl Acad Sci USA* 1997; 94: 12297–302. Available from: <http://www.pnas.org/content/94/23/12297.long>
 51. Hanes J, Pluckthun A. In vitro selection and evolution of functional proteins by using ribosome display. *Proc Natl Acad Sci USA* 1997; 94: 4937–42. Available from: <http://www.pnas.org/content/94/10/4937.long>
 52. Gai SA, Wittrup KD. Yeast surface display for protein engineering and characterization. *Curr Opin Struct Biol* 2007; 17: 467–73. Available from: <http://www.sciencedirect.com/science/article/pii/S0959440X07001194>
 53. Georgiou G, Stathopoulos C, Daugherty PS, Nayak AR, Iverson BL, Curtiss R. Display of heterologous proteins on the surface of microorganisms: from the screening of combinatorial libraries to live recombinant vaccines. *Nat Biotechnol* 1997; 15: 29–34. Available from: <http://www.nature.com/nbt/journal/v15/n1/full/nbt0197-29.html>
 54. Smith GP. Filamentous phage – novel expression vectors that display cloned antigens on the virion surface. *Science* 1985; 228: 1315–17. Available from: <http://www.jstor.org/stable/view/1694587>
 55. Hoogenboom HR. Overview of antibody phage-display technology and its applications. *Methods Mol Biol* 2002; 178: 1–37. Available from: <http://www.ncbi.nlm.nih.gov/pubmed/11968478>
 56. Lipovsek D, Pluckthun A. In-vitro protein evolution by ribosome display and mRNA display. *J Immunol Methods* 2004; 290: 51–67. Available from: <http://www.sciencedirect.com/science/article/pii/S0022175904001309>
 57. Thie H, Voedisch B, Dubel S, Hust M, Schirrmann T. Affinity maturation by phage display. *Methods Mol Biol* 2009; 525: 309–22, xv. Available from: <http://www.springerlink.com/content/1232242669467g17/?MUD=MP>
 58. Voller A, Bartlett A, Bidwell DE. Enzyme immunoassays with special reference to ELISA techniques. *J Clin Pathol* 1978; 31: 507–20. Available from: <http://jcp.bmj.com/content/31/6/507.long>
 59. Webster R. Filamentous phage biology. In: Barbas CF, Scott JK, Silverman G, eds. *Phage display: a laboratory manual*. Cold Spring Harbor, NY: Cold Spring Harbor Laboratory Press; 2001. p. 1–37.
 60. O'Connell D, Becerril B, Roy-Burman A, Daws M, Marks JD. Phage versus phagemid libraries for generation of human monoclonal antibodies. *J Mol Biol* 2002; 321: 49–56. Available from: <http://www.sciencedirect.com/science/article/pii/S0022283602005612>
 61. Hoogenboom HR, de Bruine AP, Hufton SE, Hoet RM, Arends JW, Roovers RC. Antibody phage display technology and its applications. *Immunotechnology* 1998; 4: 1–20.

- Available from: <http://www.sciencedirect.com/science/article/pii/S1380293398000074>
62. Gao C, Mao S, Lo CH, Wirsching P, Lerner RA, Janda KD. Making artificial antibodies: a format for phage display of combinatorial heterodimeric arrays. *Proc Natl Acad Sci USA* 1999; 96: 6025–30. Available from: <http://www.pnas.org/content/96/11/6025.long>
 63. Gao C, Mao S, Kaufmann G, Wirsching P, Lerner RA, Janda KD. A method for the generation of combinatorial antibody libraries using pIX phage display. *Proc Natl Acad Sci USA* 2002; 99: 12612–6. Available from: <http://www.pnas.org/content/99/20/12612.long>
 64. Shi L, Wheeler JC, Sweet RW, Lu J, Luo J, Tornetta M, et al. De novo selection of high-affinity antibodies from synthetic fab libraries displayed on phage as pIX fusion proteins. *J Mol Biol* 2010; 397: 385–96. Available from: <http://www.sciencedirect.com/science/article/pii/S002228361000080X>
 65. Kristensen P, Winter G. Proteolytic selection for protein folding using filamentous bacteriophages. *Fold Des* 1998; 3: 321–8. Available from: <http://www.sciencedirect.com/science/article/pii/S1359027898000443>
 66. de Wildt RM, Mundy CR, Gorick BD, Tomlinson IM. Antibody arrays for high-throughput screening of antibody-antigen interactions. *Nat Biotechnol* 2000; 18: 989–94. Available from: http://www.nature.com/nbt/journal/v18/n9/full/nbt0900_989.html
 67. Wrighton NC, Farrell FX, Chang R, Kashyap AK, Barbone FP, Mulcahy LS, et al. Small peptides as potent mimetics of the protein hormone erythropoietin. *Science* 1996; 273: 458–64. Available from: <http://www.sciencemag.org/content/273/5274/458.long>
 68. Winter G, Griffiths AD, Hawkins RE, Hoogenboom HR. Making antibodies by phage display technology. *Annu Rev Immunol* 1994; 12: 433–55. Available from: <http://www.annualreviews.org/doi/abs/10.1146/annurev.iy.12.040194.002245>
 69. Schier R, Bye J, Apell G, McCall A, Adams GP, Malmqvist M, et al. Isolation of high-affinity monomeric human anti-c-erb B-2 single chain Fv using affinity-driven selection. *J Mol Biol* 1996; 255: 28–43. Available from: <http://www.sciencedirect.com/science/article/pii/S0022283696900042>
 70. Wang JP, Liu YL, Teesalu T, Sugahara KN, Kotamrajua VR, Adams JD, et al. Selection of phage-displayed peptides on live adherent cells in microfluidic channels. *Proc Natl Acad Sci USA* 2011; 108: 6909–14. Available from: <http://www.pnas.org/content/108/17/6909.long>
 71. Kay BK, Thai S, Volgina VV. High-throughput biotinylation of proteins. *Methods Mol Biol* 2009; 498: 185–96. Available from: <http://www.springerlink.com/content/h5t6k868jn621gh4/?MUD=MP>
 72. Steiner D, Forrer P, Pluckthun A. Efficient selection of DARPin with sub-nanomolar affinities using SRP phage display. *J Mol Biol* 2008; 382: 1211–27. Available from: <http://www.sciencedirect.com/science/article/pii/S0022283608009650>
 73. Scholle MD, Kriplani U, Pabon A, Sishtla K, Glucksman MJ, Kay BK. Mapping protease substrates by using a biotinylated phage substrate library. *Chembiochem* 2006; 7: 834–8. Available from: <http://onlinelibrary.wiley.com/doi/10.1002/cbic.200500427/abstract>
 74. Foote J, Eisen HN. Breaking the affinity ceiling for antibodies and T cell receptors. *Proc Natl Acad Sci USA* 2000; 97: 10679–81. Available from: <http://www.pnas.org/content/97/20/10679.long>
 75. Batista FD, Neuberger MS. Affinity dependence of the B cell response to antigen: a threshold, a ceiling, and the importance of off-rate. *Immunity* 1998; 8: 751–9. Available from: <http://www.sciencedirect.com/science/article/pii/S1074761300805804>
 76. Schier R, McCall A, Adams GP, Marshall KW, Merritt H, Yim M, et al. Isolation of picomolar affinity anti-c-erbB-2 single-chain Fv by molecular evolution of the complementarity determining regions in the center of the antibody binding site. *J Mol Biol* 1996; 263: 551–67. Available from: <http://www.sciencedirect.com/science/article/pii/S0022283696905987>
 77. Groves M, Lane S, Douthwaite J, Lowne D, Rees DG, Edwards B, et al. Affinity maturation of phage display antibody populations using ribosome display. *J Immunol Methods* 2006; 313: 129–39. Available from: <http://www.sciencedirect.com/science/article/pii/S0022175906001049>
 78. van den Beucken T, Pieters H, Steukers M, van der Vaart M, Ladner RC, Hoogenboom HR, et al. Affinity maturation of Fab antibody fragments by fluorescent-activated cell sorting of yeast-displayed libraries. *FEBS Lett* 2003; 546: 288–94. Available from: <http://www.sciencedirect.com/science/article/pii/S0014579303006021>
 79. Kenrick SA, Daugherty PS. Bacterial display enables efficient and quantitative peptide affinity maturation. *Protein Eng Des Sel* 2010; 23: 9–17. Available from: <http://peds.oxfordjournals.org/content/23/1/9.long>
 80. Ling MM. Large antibody display libraries for isolation of high-affinity antibodies. *Comb Chem High Throughput Screen* 2003; 6: 421–32. Available from: <http://www.benthamdirect.com/content.php?CCHTS/2003/00000006/00000005/0001A.SGM>
 81. Marks JD, Griffiths AD, Malmqvist M, Clackson TP, Bye JM, Winter G. By-passing immunization: building high affinity human antibodies by chain shuffling. *Biotechnology (NY)* 1992; 10: 779–83. Available from: <http://www.nature.com/nbt/journal/v10/n7/pdf/nbt0792-779.pdf>
 82. Dyson MR, Zheng Y, Zhang C, Colwill K, Pershad K, Kay BK, et al. Mapping protein interactions by combining antibody affinity maturation and mass spectrometry. *Anal Biochem* 2011; 417: 25–35. Available from: <http://www.sciencedirect.com/science/article/pii/S0003269711003009>
 83. Brockmann EC, Akter S, Savukoski T, Huovinen T, Lehmusvuori A, Leivo J, et al. Synthetic single-framework antibody library integrated with rapid affinity maturation by VL shuffling. *Protein Eng Des Sel* 2011; 24: 691–700. Available from: <http://peds.oxfordjournals.org/content/24/9/691.long>
 84. Fitzgerald J, Leonard P, Darcy E, Danaher M, O’Kennedy R. Light-chain shuffling from an antigen-biased phage pool allows 185-fold improvement of an anti-halofuginone single-chain variable fragment. *Anal Biochem* 2011; 410: 27–33. Available from: <http://www.sciencedirect.com/science/article/pii/S0003269710007220>
 85. Jermutus L, Honegger A, Schwesinger F, Hanes J, Pluckthun A. Tailoring in vitro evolution for protein affinity or stability. *Proc Natl Acad Sci USA* 2001; 98: 75–80. Available from: <http://www.pnas.org/content/98/1/75.long>
 86. Famm K, Hansen L, Christ D, Winter G. Thermodynamically stable aggregation-resistant antibody domains through directed evolution. *J Mol Biol* 2008; 376: 926–31. Available from: <http://www.sciencedirect.com/science/article/pii/S0022283607014349>
 87. Cadwell RC, Joyce GF. Randomization of genes by PCR mutagenesis. *PCR Methods Appl* 1992; 2: 28–33. Available from: <http://genome.csh.org/content/2/1/28.long>
 88. Zaccolo M, Williams DM, Brown DM, Gherardi E. An approach to random mutagenesis of DNA using mixtures of triphosphate derivatives of nucleoside analogues. *J Mol Biol* 1996; 255: 589–603. Available from: <http://www.sciencedirect.com/science/article/pii/S1046202305000162>

89. Yang WP, Green K, Pinzsweney S, Briones AT, Burton DR, Barbas CF. CDR walking mutagenesis for the affinity maturation of a potent human anti-HIV-1 Antibody into the picomolar range. *J Mol Biol* 1995; 254: 392–403. Available from: <http://www.sciencedirect.com/science/article/pii/S0022283685706262>
90. McCafferty J, Griffiths AD, Winter G, Chiswell DJ. Phage antibodies: filamentous phage displaying antibody variable domains. *Nature* 1990; 348: 552–4. Available from: <http://www.nature.com/nature/journal/v348/n6301/abs/348552a0.html>
91. Thie H, Meyer T, Schirrmann T, Hust M, Dubel S. Phage display derived therapeutic antibodies. *Curr Pharm Biotechnol* 2008; 9: 439–46. Available from: <http://www.benthamdirect.org/pages/content.php?CPB/2008/00000009/00000006/0004G.SGM>
92. Nelson AL, Dhimolea E, Reichert JM. Development trends for human monoclonal antibody therapeutics. *Nat Rev Drug Discov* 2010; 9: 767–74. Available from: <http://www.nature.com/nrd/journal/v9/n10/full/nrd3229.html>
93. Rau R. Adalimumab (a fully human anti-tumour necrosis factor alpha monoclonal antibody) in the treatment of active rheumatoid arthritis: the initial results of five trials. *Ann Rheum Dis* 2002; 61(Suppl 2): ii70–3.
94. Abbott drug tops sales as Lipitor, Plavix era ends. Available from: <http://uk.reuters.com/article/2012/04/11/uk-pharmaceuticals-abbott-idUKBRE83A0PU20120411> [cited 4 November 2012].
95. den Broeder A, van de Putte L, Rau R, Schattenkirchner M, Van Riel P, Sander O, et al. A single dose, placebo controlled study of the fully human anti-tumor necrosis factor-alpha antibody adalimumab (D2E7) in patients with rheumatoid arthritis. *J Rheumatol* 2002; 29: 2288–98. Available from: <http://ard.bmj.com/content/62/12/1168.long>
96. Osbourn J, Groves M, Vaughan T. From rodent reagents to human therapeutics using antibody guided selection. *Methods* 2005; 36: 61–8. Available from: <http://www.sciencedirect.com/science/article/pii/S1046202305000162>
97. Xian-Li H, Guo-qiang B. Guided Selection Methods Through Chain Shuffling. In: Aitken R, ed. *antibody phage display*. New York, NY: Humana Press; 2009. p. 133–42.
98. Hartmut Kupper JS, Tracey D, Kalden JR. *Handbook of therapeutic antibodies*. Hoboken, NJ: Wiley; 2008. p. 697–732.
99. Benlysta (Belimumab). Available from: <http://www.hgsi.com/benlysta-belimumab-3.html> [cited December 2011].
100. Stohl W, Hilbert DM. The discovery and development of belimumab: the anti-BLyS-lupus connection. *Nat Biotechnol* 2012; 30: 69–77. Available from: <http://www.nature.com/nbt/journal/v30/n1/full/nbt.2076.html>
101. Schiemann B, Gommerman JL, Vora K, Cachero TG, Shulgamorskaya S, Dobles M, et al. An essential role for BAFF in the normal development of B cells through a BCMA-independent pathway. *Science* 2001; 293: 2111–4. Available from: <http://www.sciencemag.org/content/293/5537/2111.short>
102. Dennis GJ. Belimumab: a BLyS-specific inhibitor for the treatment of systemic lupus erythematosus. *Clin Pharmacol Ther* 2012; 91: 143–9. Available from: <http://www.nature.com/clpt/journal/v91/n1/full/clpt2011290a.html>
103. FDA approves Benlysta to treat lupus. Available from: <http://www.fda.gov/NewsEvents/Newsroom/PressAnnouncements/ucm246489.htm> [cited December 2011]
104. Navarra SV, Guzman RM, Gallacher AE, Hall S, Levy RA, Jimenez RE, et al. Efficacy and safety of belimumab in patients with active systemic lupus erythematosus: a randomised, placebo-controlled, phase 3 trial. *Lancet* 2011; 377: 721–31. Available from: [http://www.thelancet.com/journals/lancet/article/PIIS0140-6736\(10\)61354-2/fulltext](http://www.thelancet.com/journals/lancet/article/PIIS0140-6736(10)61354-2/fulltext)
105. Baker KP, Edwards BM, Main SH, Choi GH, Wager RE, Halpern WG, et al. Generation and characterization of LymphoStat-B, a human monoclonal antibody that antagonizes the bioactivities of B lymphocyte stimulator. *Arthritis Rheum* 2003; 48: 3253–65. Available from: <http://onlinelibrary.wiley.com/doi/10.1002/art.11299/abstract;jsessionid=3544747B23B8B065F8A05B519826EACC.d02i04>
106. Illumina. Available from: <http://www.illumina.com> [cited April 2012].
107. Heller MJ. DNA microarray technology: devices, systems, and applications. *Annu Rev Biomed Eng* 2002; 4: 129–53. Available from: <http://www.annualreviews.org/doi/full/10.1146/annurev.bioeng.4.020702.153438>
108. Ramachandran N, Srivastava S, Labaer J. Applications of protein microarrays for biomarker discovery. *Proteomics Clin Appl* 2008; 2: 1444–59. Available from: <http://onlinelibrary.wiley.com/doi/10.1002/prca.200800032/abstract>
109. Weber A, Henge UR, Stricker I, Tischoff I, Markwart A, Anhalt K, et al. Protein microarrays for the detection of biomarkers in head and neck squamous cell carcinomas. *Hum Pathol* 2007; 38: 228–38. Available from: <http://www.sciencedirect.com/science/article/pii/S004681770600459X>
110. Acevedo B, Perera Y, Ruiz M, Rojas G, Benitez J, Ayala M, et al. Development and validation of a quantitative ELISA for the measurement of PSA concentration. *Clin Chim Acta* 2002; 317: 55–63. Available from: <http://www.sciencedirect.com/science/article/pii/S0009898101007495>
111. Mishra J, Dent C, Tarabishi R, Mitsnefes MM, Ma Q, Kelly C, et al. Neutrophil gelatinase-associated lipocalin (NGAL) as a biomarker for acute renal injury after cardiac surgery. *Lancet* 2005; 365: 1231–38. Available from: <http://www.sciencedirect.com/science/article/pii/S014067360574811X>
112. Diamandis EP. Mass spectrometry as a diagnostic and a cancer biomarker discovery tool – opportunities and potential limitations. *Mol Cell Proteomics* 2004; 3: 367–78. Available from: <http://www.mcponline.org/content/3/4/367.full>
113. Kim SN, Rusling JF, Papadimitrakopoulos F. Carbon nanotubes for electronic and electrochemical detection of biomolecules. *Adv Mater* 2007; 19: 3214–28. Available from: <http://onlinelibrary.wiley.com/doi/10.1002/adma.200700665/abstract>
114. O'Connor M, Kim SN, Killard AJ, Forster RJ, Smyth MR, Papadimitrakopoulos F, et al. Mediated amperometric immunosensing using single walled carbon nanotube forests. *Analyst* 2004; 129: 1176–80. Available from: <http://pubs.rsc.org/en/Content/ArticleLanding/2004/AN/b412805b>
115. Rusling JF, Munge BS, Krause CE, Malhotra R, Patel V, Gutkind JS. Electrochemical immunosensors for interleukin-6. Comparison of carbon nanotube forest and gold nanoparticle platforms. *Electrochem Commun* 2009; 11: 1009–12. Available from: <http://www.sciencedirect.com/science/article/pii/S1388248109001088>
116. Riedel F, Zaiss I, Herzog D, Gotte K, Naim R, Hormann K. Serum levels of interleukin-6 in patients with primary head and neck squamous cell carcinoma. *Anticancer Res* 2005; 25: 2761–5. Available from: <http://ar.iiarjournals.org/content/25/4/2761.long>
117. Rusling JF, Malhotra R, Patel V, Vaque JP, Gutkind JS. Ultrasensitive electrochemical immunosensor for oral cancer biomarker IL-6 using carbon nanotube forest electrodes and multilabel amplification. *Anal Chem* 2010; 82: 3118–23. Available from: <http://pubs.acs.org/doi/abs/10.1021/ac902802b>
118. Rusling JF, Chikkaveeraiah BV, Bhirde A, Malhotra R, Patel V, Gutkind JS. Single-wall carbon nanotube forest arrays for immunoelectrochemical measurement of four protein biomarkers for prostate cancer. *Anal Chem* 2009; 81: 9129–34. Available from: <http://pubs.acs.org/doi/abs/10.1021/ac901802z>
119. Chen RJ, Bangsaruntip S, Drouvalakis KA, Kam NW, Shim M, Li Y, et al. Noncovalent functionalization of carbon nanotubes for highly specific electronic biosensors. *Proc Natl*

- Acad Sci USA 2003; 100: 4984–9. Available from: <http://www.pnas.org/content/100/9/4984.long>
120. Heller I, Janssens AM, Mannik J, Minot ED, Lemay SG, Dekker C. Identifying the mechanism of biosensing with carbon nanotube transistors. *Nano Lett* 2008; 8: 591–5. Available from: <http://pubs.acs.org/doi/abs/10.1021/nl072996i>
 121. Lee JO, Park DW, Kim YH, Kim BS, So HM, Won K, et al. Detection of tumor markers using single-walled carbon nanotube field effect transistors. *J Nanosci Nanotechnol* 2006; 6: 3499–502. Available from: <http://www.ingentaconnect.com/content/asp/jnn/2006/00000006/00000011/art00044>
 122. Lo YS, Nam DH, So HM, Chang H, Kim JJ, Kim YH, et al. Oriented immobilization of antibody fragments on Ni-decorated single-walled carbon nanotube devices. *ACS Nano* 2009; 3: 3649–55. Available from: <http://pubs.acs.org/doi/abs/10.1021/nn900540a>
 123. Wang CW, Pan CY, Wu HC, Shih PY, Tsai CC, Liao KT, et al. In situ detection of chromogranin a released from living neurons with a single-walled carbon-nanotube field-effect transistor. *Small* 2007; 3: 1350–5. Available from: <http://onlinelibrary.wiley.com/doi/10.1002/sml.200600723/abstract>
 124. Lerner MB, D'Souza J, Pazina T, Dailey J, Goldsmith BR, Robinson MK, et al. Hybrids of a genetically engineered antibody and a carbon nanotube transistor for detection of prostate cancer biomarkers. *ACS Nano* 2012; 6: 5143–5149. Available from: <http://pubs.acs.org/doi/full/10.1021/nn300819s>
 125. Weber GF, Lett GS, Haubein NC. Osteopontin is a marker for cancer aggressiveness and patient survival. *Br J Cancer* 2010; 103: 861–9. Available from: <http://www.nature.com/bjc/journal/v103/n6/full/6605834a.html>
 126. Raman CV, Krishnan KS. A new type of secondary radiation (Reprinted from *Nature* 1928; 121: 501–2). *Curr Sci* 1998; 74: 381. Available from: http://www.ias.ac.in/j_archive/currsci/74/4/381-381/viewpage.html
 127. Raman ICV. A change of wave-length in light scattering. *Nature* 1928; 121: 465–6.
 128. Landsberg G, Mandelstam L. Eine neue Erscheinung bei der Lichtzerstreuung in Krystallen. *Naturwissenschaften* 1928; 16: 557–8.
 129. Fleischmann M, Hendra PJ, McQuilla AJ. Raman-spectra of pyridine adsorbed at a silver electrode. *Chem Phys Lett* 1974; 26: 163–6. Available from: <http://www.sciencedirect.com/science/article/pii/0009261474853881>
 130. Jeanmaire DL, van Duyne RP. Surface raman electrochemistry part I. Heterocyclic, aromatic and aliphatic amines adsorbed on the anodized silver electrode. *J Electroanal Chem* 1977; 84: 1–20.
 131. Albrecht MG, Creighton JA. Anomalously intense raman-spectra of pyridine at a silver electrode. *J Am Chem Soc* 1977; 99: 5215–7. Available from: <http://pubs.acs.org/doi/abs/10.1021/ja00457a071>
 132. Porter MD, Ni J, Lipert RJ, Dawson GB. Immunoassay readout method using extrinsic Raman labels adsorbed on immunogold colloids. *Anal Chem* 1999; 71: 4903–8. Available from: <http://pubs.acs.org/doi/abs/10.1021/ac990616a>
 133. Mirkin CA, Cao YC, Jin RC, Thaxton CS. Raman dye-labeled nanoparticle probes for proteins. *J Am Chem Soc* 2003; 125: 14676–7. Available from: <http://pubs.acs.org/doi/pdfplus/10.1021/ja0366235>
 134. Schlücker S, Kiefer W. Selective Detection of Proteins and Nucleic Acids with Biofunctionalized eds. *Frontiers of Molecular Spectroscopy*. Amsterdam, Netherlands: Elsevier; 2009. p. 267–88.
 135. Chon H, Lee S, Son SW, Oh CH, Choo J. Highly sensitive immunoassay of lung cancer marker carcinoembryonic antigen using surface-enhanced Raman scattering of hollow gold nanospheres. *Anal Chem* 2009; 81: 3029–34. Available from: <http://pubs.acs.org/doi/abs/10.1021/ac802722c>
 136. Lee M, Lee S, Lee JH, Lim HW, Seong GH, Lee EK, et al. Highly reproducible immunoassay of cancer markers on a gold-patterned microarray chip using surface-enhanced Raman scattering imaging. *Biosens Bioelectron* 2011; 26: 2135–41. Available from: <http://www.sciencedirect.com/science/article/pii/S0956566310006342>
 137. Bishnoi SW, Lin YJ, Tibudan M, Huang YM, Nakaema M, Swarup V, et al. SERS biodetection using gold-silica nanoshells and nitrocellulose membranes. *Anal Chem* 2011; 83: 4053–60. Available from: <http://pubs.acs.org/doi/abs/10.1021/ac103195e>
 138. Qian X, Peng XH, Ansari DO, Yin-Goen Q, Chen GZ, Shin DM, et al. In vivo tumor targeting and spectroscopic detection with surface-enhanced Raman nanoparticle tags. *Nat Biotechnol* 2008; 26: 83–90. Available from: <http://www.nature.com/nbt/journal/v26/n1/full/nbt1377.html>
 139. Holmes JD, Johnston KP, Doty RC, Korgel BA. Control of thickness and orientation of solution-grown silicon nanowires. *Science* 2000; 287: 1471–3. Available from: <http://www.sciencemag.org/content/287/5457/1471.short>
 140. Lieber CM. One-dimensional nanostructures: chemistry, physics & applications. *Solid State Commun* 1998; 107: 607–16. Available from: <http://www.sciencedirect.com/science/article/pii/S0038109898002099>
 141. Jeyakumar Ramanujam, Shri D, Verma A. Silicon nanowire growth and properties: a review. *Mater Express* 2011; 1: 105–26. Available from: <http://www.ingentaconnect.com/content/asp/me/2011/00000001/00000002/art00002>
 142. Stucky GD, MacDougall JE. Quantum confinement and host/guest chemistry: probing a new dimension. *Science* 1990; 247: 669–78. Available from: <http://www.sciencemag.org/content/247/4943/669.long>
 143. Ramgir NS, Yang Y, Zacharias M. Nanowire-based sensors. *Small* 2010; 6: 1705–22. Available from: <http://onlinelibrary.wiley.com/doi/10.1002/sml.201000972/abstract>
 144. Lieber CM, Zheng GF, Patolsky F, Cui Y, Wang WU. Multiplexed electrical detection of cancer markers with nanowire sensor arrays. *Nat Biotechnol* 2005; 23: 1294–301. Available from: <http://www.nature.com/nbt/journal/v23/n10/full/nbt1138.html>
 145. Medintz IL, Uyeda HT, Goldman ER, Mattoussi H. Quantum dot bioconjugates for imaging, labelling and sensing. *Nat Mater* 2005; 4: 435–46. Available from: <http://www.nature.com/nmat/journal/v4/n6/full/nmat1390.html>
 146. Rosenthal SJ, Chang JC, Kovtun O, McBride JR, Tomlinson ID. Biocompatible quantum dots for biological applications. *Chem Biol* 2011; 18: 10–24. Available from: <http://www.sciencedirect.com/science/article/pii/S1074552110004497>
 147. Kippenny T, Swafford LA, Rosenthal SJ. Semiconductor nanocrystals: a powerful visual aid for introducing the particle in a box. *J Chem Educ* 2002; 79: 1094–100. Available from: <http://pubs.acs.org/doi/abs/10.1021/ed079p1094>
 148. Barroso MM. Quantum dots in cell biology. *J Histochem Cytochem* 2011; 59: 237–51. Available from: <http://jhc.sagepub.com/content/59/3/237>
 149. Resch-Genger U, Grabolle M, Cavaliere-Jaricot S, Nitschke R, Nann T. Quantum dots versus organic dyes as fluorescent labels. *Nat Methods* 2008; 5: 763–75. Available from: <http://www.nature.com/nmeth/journal/v5/n9/full/nmeth.1248.html>
 150. Barat B, Sirk SJ, McCabe KE, Li J, Lepin EJ, Remenyi R, et al. Cys-diabody quantum dot conjugates (immunoQdots) for cancer marker detection. *Bioconjug Chem* 2009; 20: 1474–81. Available from: <http://pubs.acs.org/doi/abs/10.1021/bc800421f>
 151. Yokota T, Milenic DE, Whitlow M, Schlom J. Rapid tumor penetration of a single-chain Fv and comparison with other

- immunoglobulin forms. *Cancer Res* 1992; 52: 3402–8. Available from: <http://cancerres.aacrjournals.org/content/52/12/3402.long>
152. Mattheakis LC, Dias JM, Choi YJ, Gong J, Bruchez MP, Liu JQ, et al. Optical coding of mammalian cells using semiconductor quantum dots. *Anal Biochem* 2004; 327: 200–8. Available from: <http://www.sciencedirect.com/science/article/pii/S0003269704000764>
 153. Saerens D, Kinne J, Bosmans E, Wernery U, Muyldermans S, Conrath K. Single domain antibodies derived from dromedary lymph node and peripheral blood lymphocytes sensing conformational variants of prostate-specific antigen. *J Biol Chem* 2004; 279: 51965–72. Available from: <http://www.jbc.org/content/279/50/51965.long>
 154. Whitfield D, Zaman MB, Baral TN, Zhang JB, Yu K. Single-domain antibody functionalized CdSe/ZnS quantum dots for cellular imaging of cancer cells. *J Phys Chem C* 2009; 113: 496–9. Available from: <http://pubs.acs.org/doi/abs/10.1021/jp809159k>
 155. Balalaeva IV, Zdobnova TA, Brilkina AA, Krutova IM, Stremovskiy OA, Lebedenko EN, et al. Whole-body imaging of HER2/neu-overexpressing tumors using scFv-antibody conjugated quantum dots. *Proc SPIE* 2010; 7575: 757510. Available from: http://spiedigitallibrary.org/proceedings/resource/2/psidg/7575/1/757510_1?isAuthorized=no
 156. Sauerbrey G. Verwendung von Schwingquarzen zur Wägung dünner Schichten und zur Mikrowägung. *Zeitschrift für Physik* 1959; 155: 206–22.
 157. Uludag Y, Tothill IE. Development of a sensitive detection method of cancer biomarkers in human serum (75%) using a quartz crystal microbalance sensor and nanoparticles amplification system. *Talanta* 2010; 82: 277–82. Available from: <http://www.sciencedirect.com/science/article/pii/S0039914010002912>
 158. Shen Z, Mernaugh RL, Yan H, Yu L, Zhang Y, Zeng X. Engineered recombinant single-chain fragment variable antibody for immunosensors. *Anal Chem* 2005; 77: 6834–42. Available from: <http://pubs.acs.org/doi/abs/10.1021/ac0507690>
 159. Kroger D, Liley M, Schiweck W, Skerra A, Vogel H. Immobilization of histidine-tagged proteins on gold surfaces using chelator thioalkanes. *Biosens Bioelectron* 1999; 14: 155–61. Available from: <http://www.sciencedirect.com/science/article/pii/S095656639800116X>
 160. Shen Z, Yan H, Parl FF, Mernaugh RL, Zeng X. Recombinant antibody piezoimmunosensors for the detection of cytochrome P450 1B1. *Anal Chem* 2007; 79: 1283–9. Available from: <http://pubs.acs.org/doi/abs/10.1021/ac061211a>
 161. Dill K, Montgomery DD, Ghindilis AL, Schwarzkopf KR, Ragsdale SR, Oleinikov AV. Immunoassays based on electrochemical detection using microelectrode arrays. *Biosens Bioelectron* 2004; 20: 736–42. Available from: <http://www.sciencedirect.com/science/article/pii/S0038109898002099>
 162. Korri-Yousoufi H, Le HQA, Sauriat-Dorizon H. Investigation of SPR and electrochemical detection of antigen with polypyrrole functionalized by biotinylated single-chain antibody: a review. *Anal Chim Acta* 2010; 674: 1–8. Available from: <http://www.sciencedirect.com/science/article/pii/S0003267010007464>
 163. Wang J. Electrochemical biosensors: towards point-of-care cancer diagnostics. *Biosens Bioelectron* 2006; 21: 1887–92. Available from: <http://www.sciencedirect.com/science/article/pii/S0956566305003441>
 164. Oleinikov AV, Gray MD, Zhao J, Montgomery DD, Ghindilis AL, Dill K. Self-assembling protein arrays using electronic semiconductor microchips and in vitro translation. *J Proteome Res* 2003; 2: 313–9. Available from: <http://pubs.acs.org/doi/abs/10.1021/pr0300011>
 165. Bailey RC, Kwong GA, Radu CG, Witte ON, Heath JR. DNA-encoded antibody libraries: a unified platform for multiplexed cell sorting and detection of genes and proteins. *J Am Chem Soc* 2007; 129: 1959–67. Available from: <http://pubs.acs.org/doi/abs/10.1021/ja065930i>
 166. Hwang KS, Lee SM, Kim SK, Lee JH, Kim TS. Micro- and nanocantilever devices and systems for biomolecule detection. *Annu Rev Anal Chem (Palo Alto Calif)* 2009; 2: 77–98. Available from: <http://www.annualreviews.org/doi/full/10.1146/annurev-anchem-060908-155232>
 167. Burg TP, Mirza AR, Milovic N, Tsau CH, Popescu GA, Foster JS, et al. Vacuum-packaged suspended micro-channel resonant mass sensor for biomolecular detection. *J Microelectromech Syst* 2006; 15: 1466–76. Available from: http://ieeexplore.ieee.org/xpl/articleDetails.jsp?tp=&arnumber=4020254&contentType=Journals+%26+Magazines&sortType%3Dasc_p_Sequence%26filter%3DAND%28p_IS_Number%3A4020250%29
 168. Wu G, Datar RH, Hansen KM, Thundat T, Cote RJ, Majumdar A. Bioassay of prostate-specific antigen (PSA) using microcantilevers. *Nat Biotechnol* 2001; 19: 856–60. Available from: <http://www.nature.com/nbt/journal/v19/n9/full/nbt0901-856.html>
 169. Kim TS, Lee JH, Hwang KS, Park J, Yoon KH, Yoon DS. Immunoassay of prostate-specific antigen (PSA) using resonant frequency shift of piezoelectric nanomechanical microcantilever. *Biosens Bioelectron* 2005; 20: 2157–62. Available from: <http://www.sciencedirect.com/science/article/pii/S0956566304004488>
 170. Adams GP, Loo L, Capobianco JA, Wu W, Gao XT, Shih WY, et al. Highly sensitive detection of HER2 extracellular domain in the serum of breast cancer patients by piezoelectric microcantilevers. *Anal Chem* 2011; 83: 3392–7. Available from: <http://pubs.acs.org/doi/abs/10.1021/ac103301r>
 171. SRU Biosystems. Available from: <http://www.srubiosystems.com/> [cited May 2012].
 172. Cunningham BT, Li P, Schulz S, Lin B, Baird C, Gerstenmaier J, et al. Label-free assays on the BIND system. *J Biomol Screen* 2004; 9: 481–90. Available from: <http://jbx.sagepub.com/content/9/6/481.long>
 173. Huang CS, George S, Lu M, Chaudhery V, Tan RM, Zangar RC, et al. Application of photonic crystal enhanced fluorescence to cancer biomarker microarrays. *Anal Chem* 2011; 83: 1425–30. Available from: <http://pubs.acs.org/doi/abs/10.1021/ac102989n>
 174. Chen R, Mias GI, Li-Pook-Tham J, Jiang L, Lam HY, Miriami E, et al. Personal omics profiling reveals dynamic molecular and medical phenotypes. *Cell* 2012; 148: 1293–307. Available from: [http://www.cell.com/fulltext/S0092-8674\(12\)00166-3](http://www.cell.com/fulltext/S0092-8674(12)00166-3)

***Brian K. Kay**

Department of Biological Sciences
 University of Illinois at Chicago (UIC)
 845 W. Taylor St.
 3240 SES MC 066
 Chicago
 IL 60607-7060
 USA
 Tel: 01-312-996-4249
 Email: bkay@uic.edu